

Supplementary Information

Synergistic or Antagonistic Antioxidant Combinations - A Case Study Exploring Flavonoid-Nitroxides Hybrids

Astrid C. R. Larin, Michael C. Pfrunder, Kathleen M. Mullen, Sandra Wiedbrauk, Nathan R. Boase, and Kathryn E. Fairfull-Smith

Contents

Synthesis.....	2
2-Acetylphenyl 2-methoxy-1,1,3,3-tetramethylisoindoline-5-carboxylate (12)	2
1-(2-Hydroxyphenyl)-3-(2-methoxy-1,1,3,3-tetramethylisoindolin-5-yl)propane-1,3-dione (13)	6
2-(2-Methoxy-1,1,3,3-tetramethylisoindolin-5-yl)-4H-chrome n-4-one (14)	10
2-(2-Methoxy-1,1,3,3-tetramethylisoindolin-5-yl)-3-(2-methoxy-1,1,3,3-tetramethylisoindoline-5-carbonyl)-4H-chromen-4-one (15).....	14
2-(1,1,3,3-Tetramethylisoindolin-2-oxyl)-4H-chromen-4-one (6).....	18
2-(1,1,3,3-Tetramethylisoindolin-2-oxyl)-3-(1,1,3,3-tetramethylisoindolin-2-oxyl-5-carbonyl)-4H-chromen-4-one (8).....	22
2-Acetyl-3-hydroxyphenyl 2-methoxy-1,1,3,3-tetramethylisoindoline-5-carboxylate (17).....	26
5-Hydroxy-2-(2-methoxy-1,1,3,3-tetramethylisoindolin-5-yl)-4H-chromen-4-one (18).....	30
2-Acetyl-1,3-phenylene bis(2-methoxy-1,1,3,3-tetramethylisoindoline-5-carboxylate) (19)	34
5-Hydroxy-2-(2-methoxy-1,1,3,3-tetramethylisoindolin-5-yl)-3-(2-methoxy-1,1,3,3-tetramethylisoindoline-5-carbonyl)-4H-chromen-4-one (20)	38
5-Hydroxy-2-(1,1,3,3-tetramethylisoindolin-2-oxyl)-4H-chromen-4-one (7)	42
5-Hydroxy-2-(1,1,3,3-tetramethylisoindolin-2-oxyl)-3-(1,1,3,3-tetramethylisoindolin-2-oxyl-5-carbonyl)-4H-chromen-4-one (9).....	47
Single Crystal X-ray Diffraction Experimental	52
Cyclic voltammograms of 5-OH Flavone and 5-OH-3-Benzoyl flavone series	54
Oxygen Radical Antioxidant Capacity (ORAC) Data	55
ORAC assay followed by EPR and fluorescence spectroscopy.....	58
EPR spectra of compounds (1, 6 and 7) in various solvents	59
References	60

Synthesis

2-Acetylphenyl 2-methoxy-1,1,3,3-tetramethylisoindoline-5-carboxylate (12)

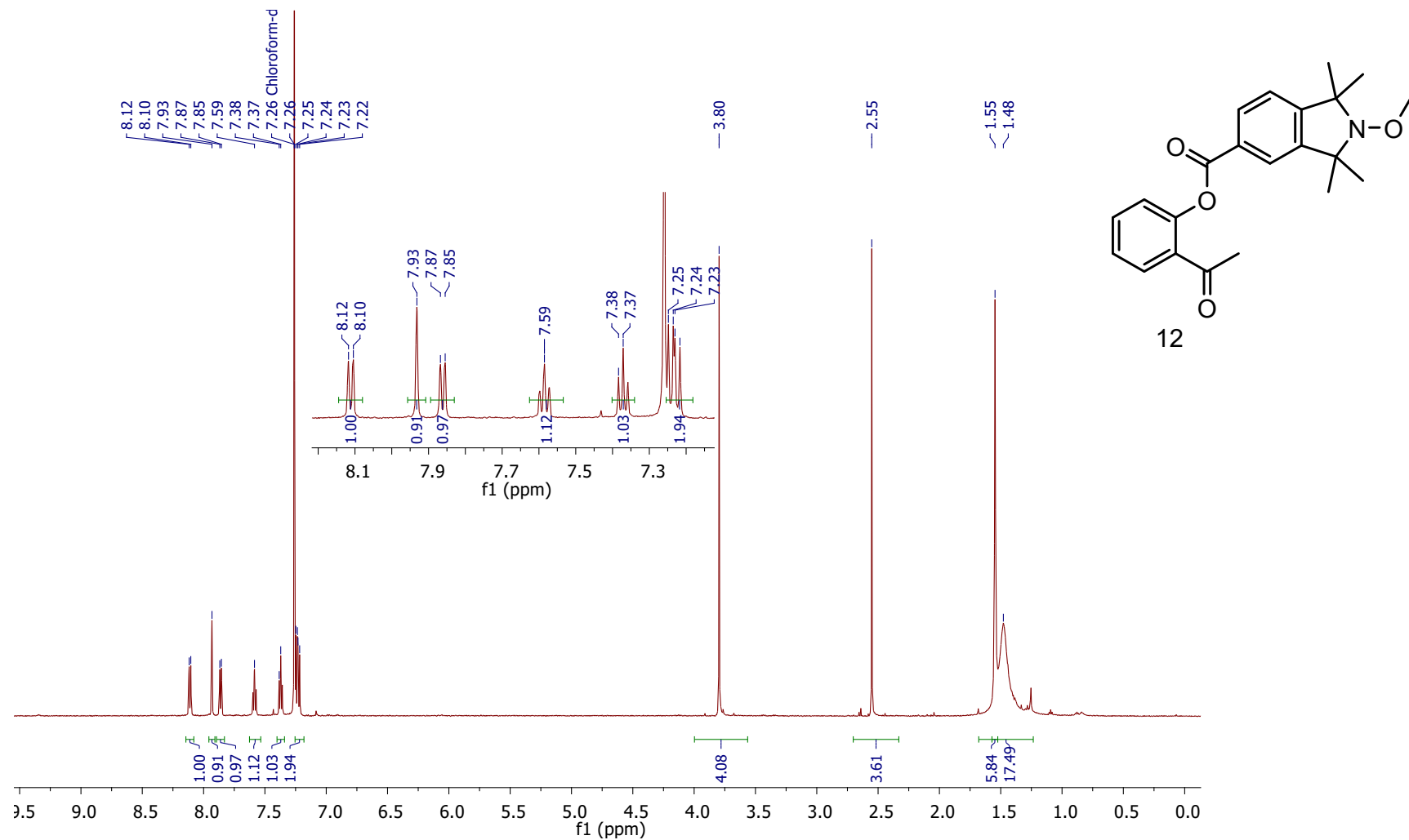
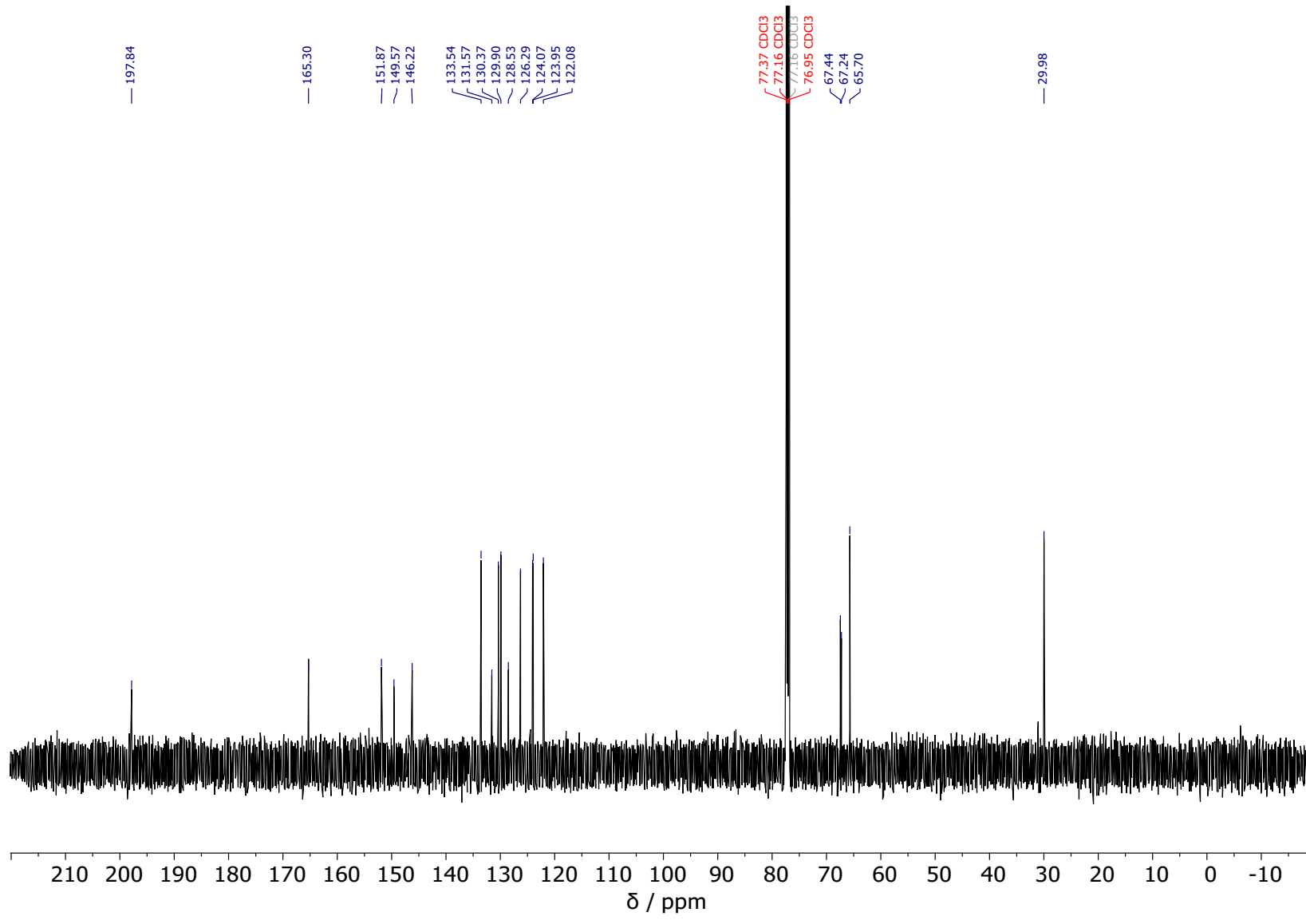


Figure S1: ¹H NMR spectrum of **12** (CDCl₃, 600 MHz).



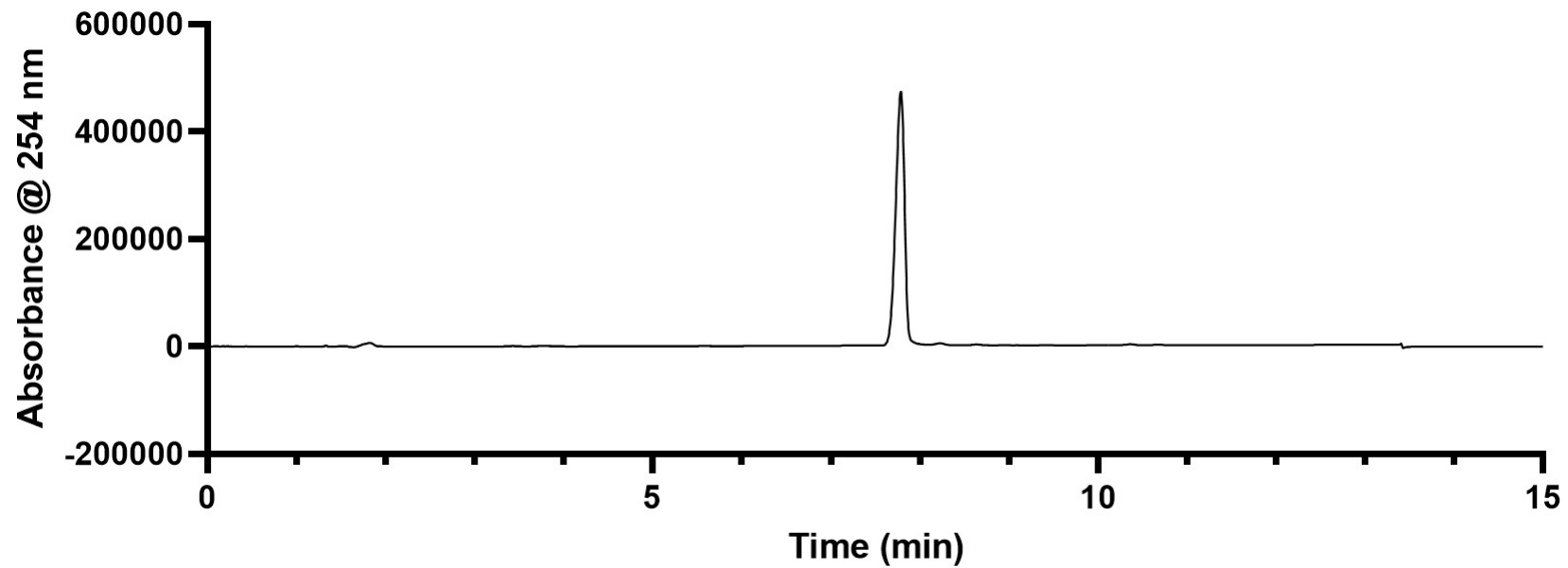


Figure S3: LC trace (215 nm detector wavelength) of **12**. The gradient was altered for this compound to ACN:H₂O (0.1% formic acid) 10:90 – 80:20.

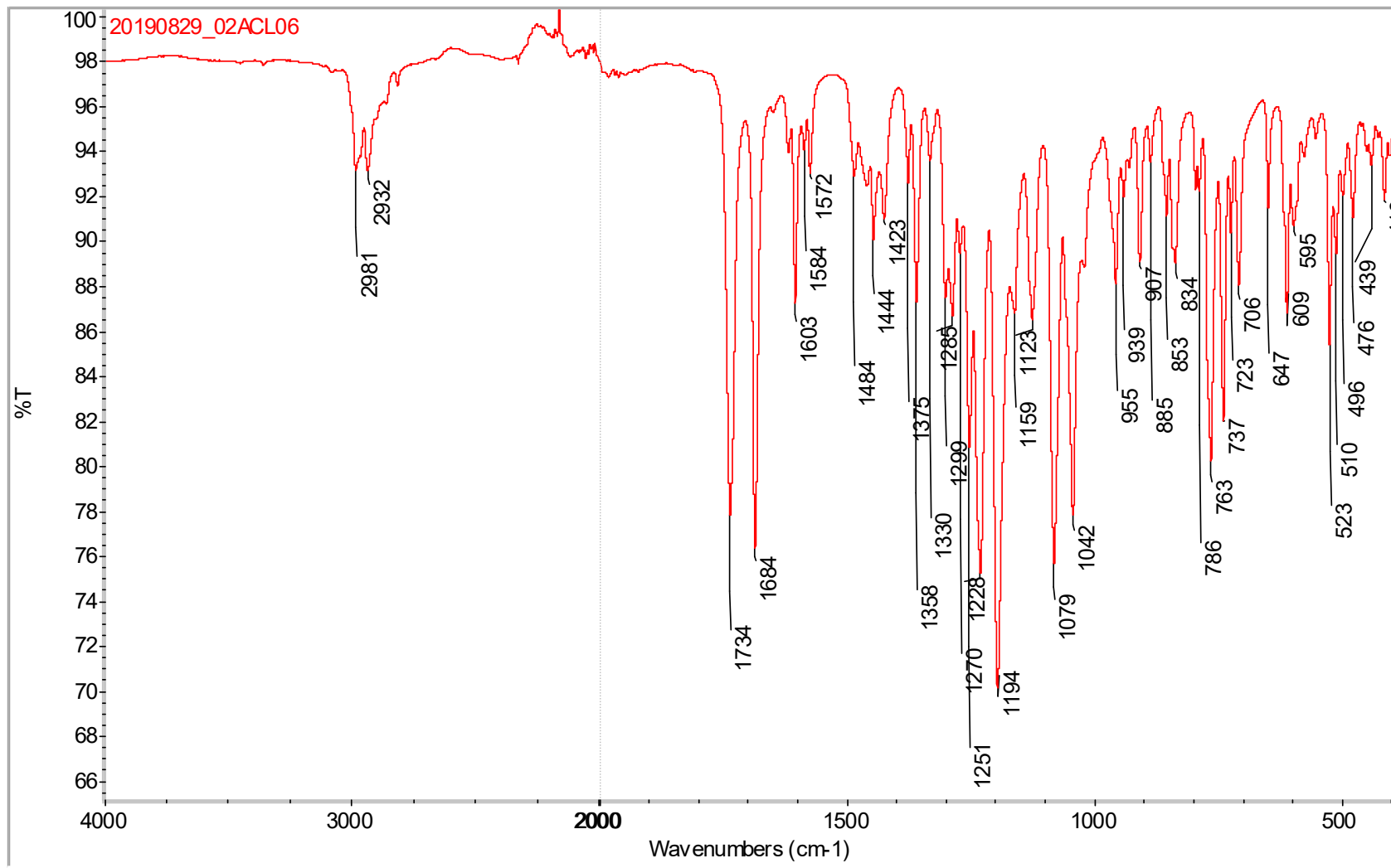


Figure S4: FT-IR spectrum of **12**.

1-(2-Hydroxyphenyl)-3-(2-methoxy-1,1,3,3-tetramethylisoindolin-5-yl)propane-1,3-dione (**13**)

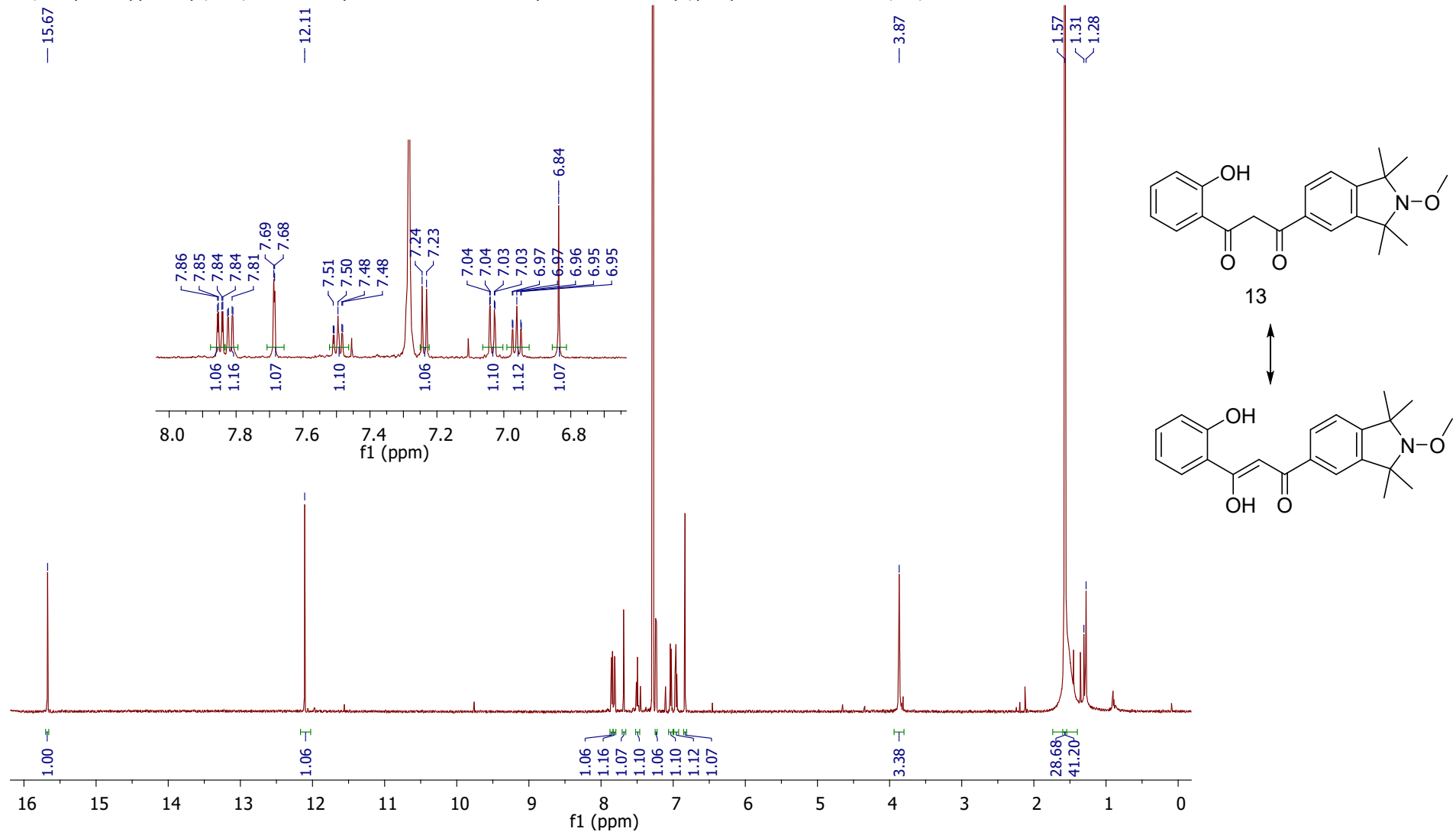


Figure S5: ¹H NMR spectrum of **13** (CDCl₃, 600 MHz).

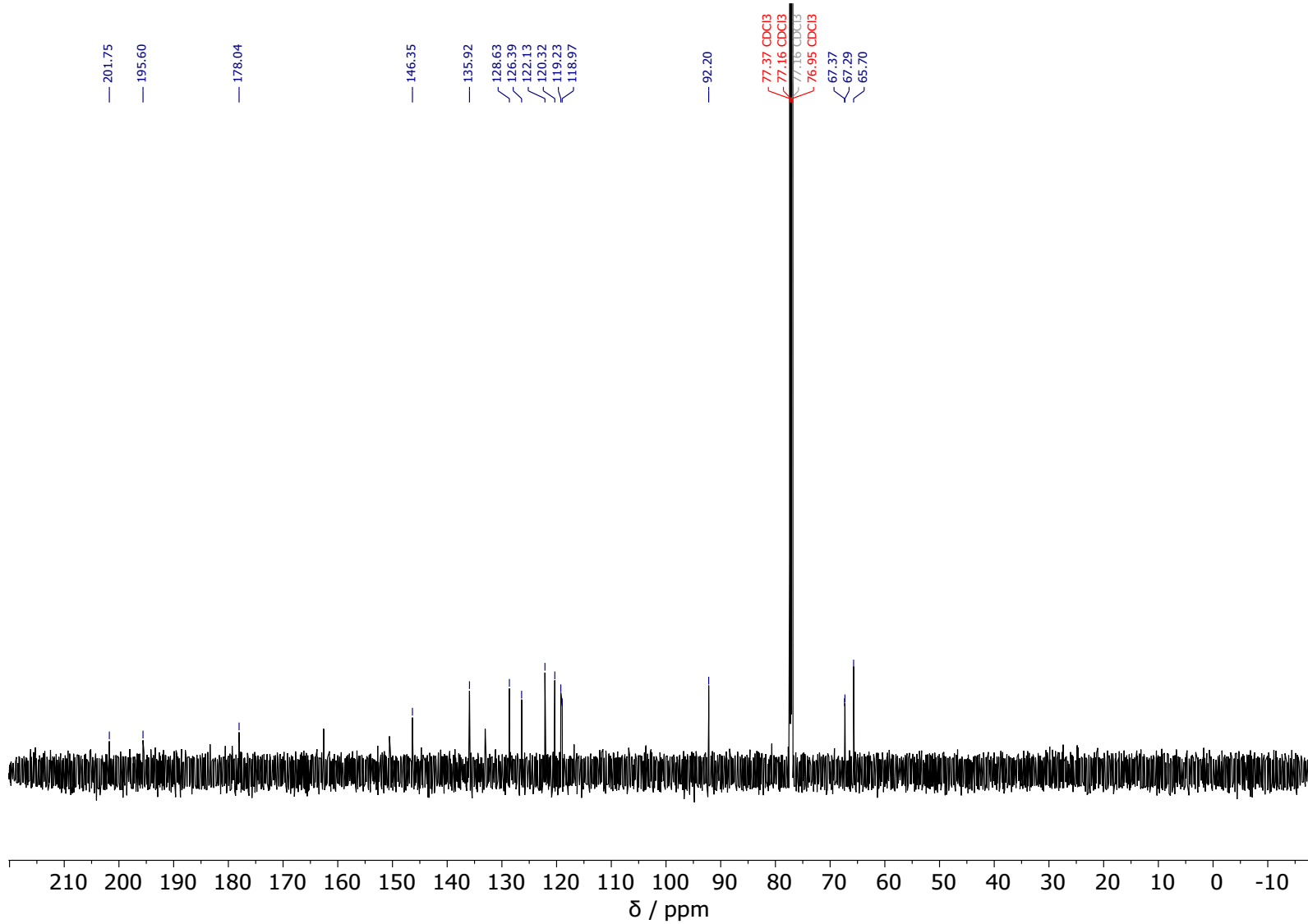


Figure S6: ^{13}C NMR spectrum of **13** (CDCl_3 , 151 MHz).

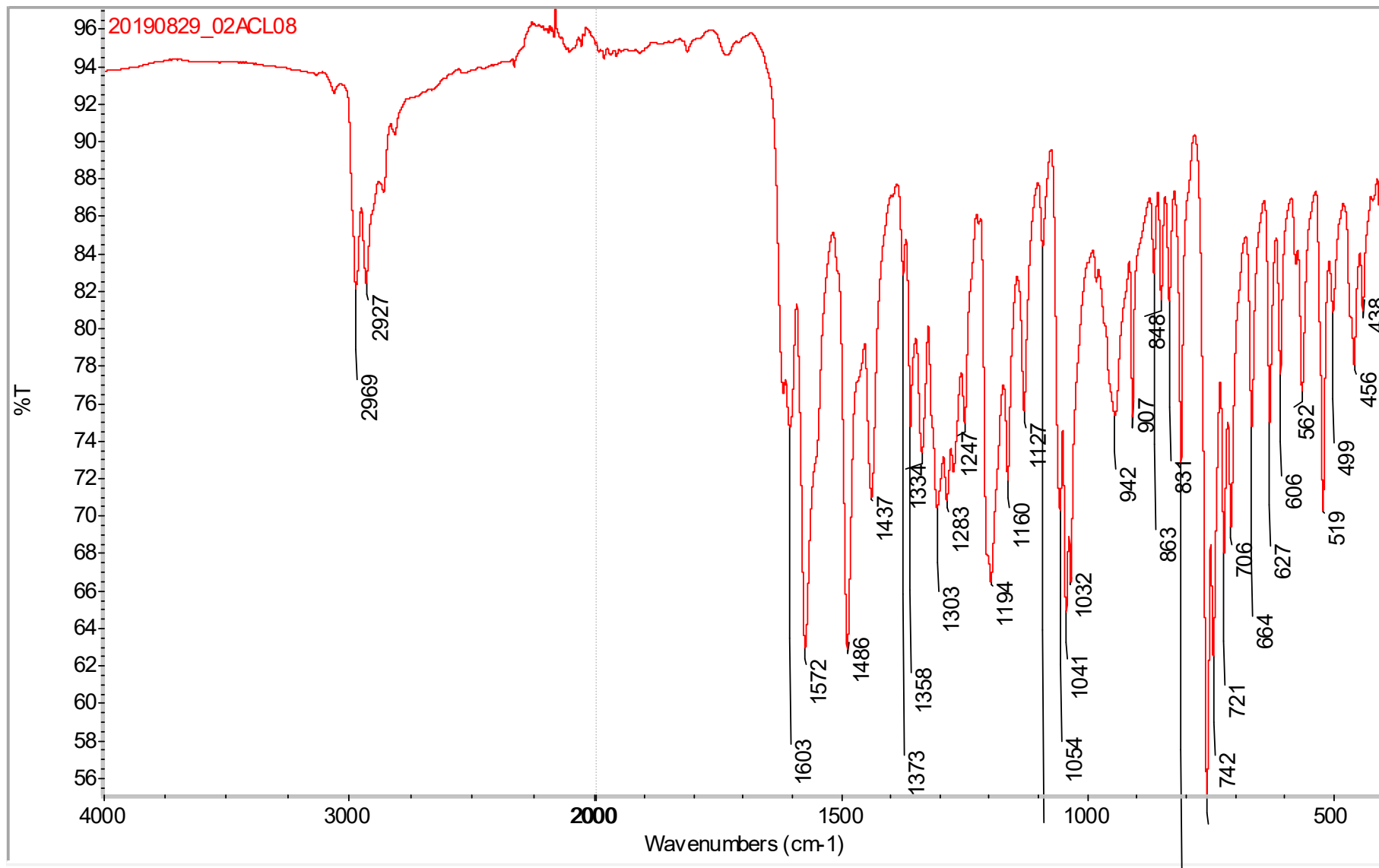


Figure S7: FT-IR Spectrum of **13**

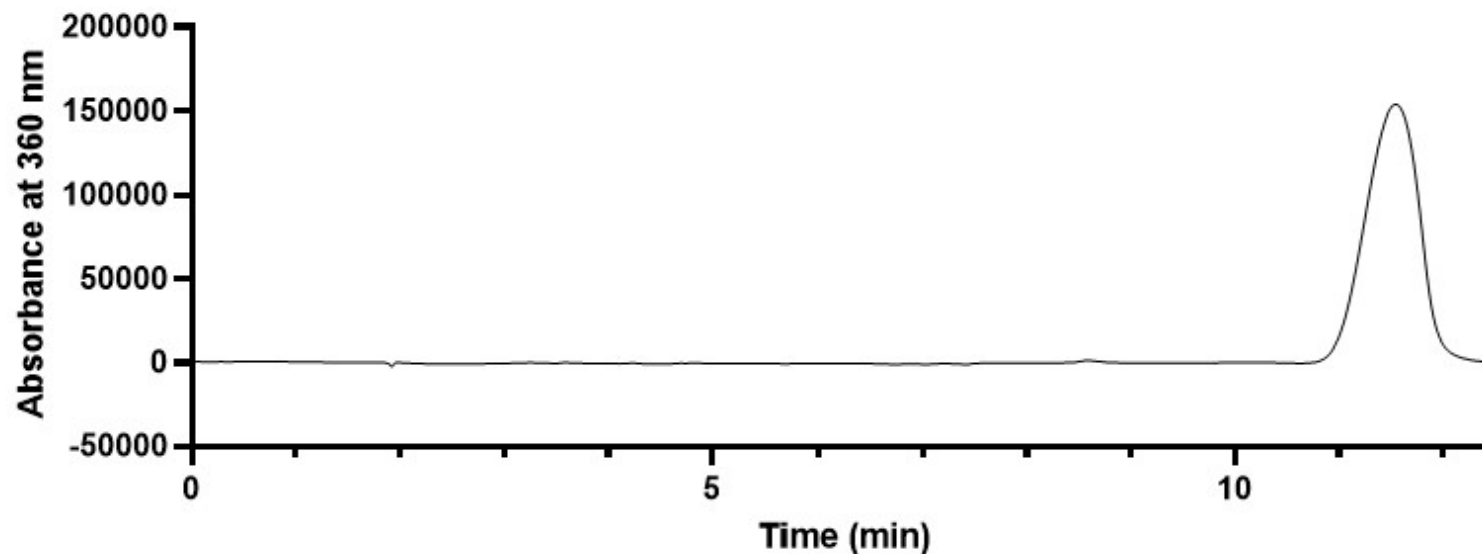


Figure S8: LC trace (360 nm detector wavelength) of **13**. The gradient was altered for this compound to ACN:H₂O (0.1% formic acid) 10:90 – 80:20.

2-(2-Methoxy-1,1,3,3-tetramethylisoindolin-5-yl)-4H-chrome n-4-one (**14**)

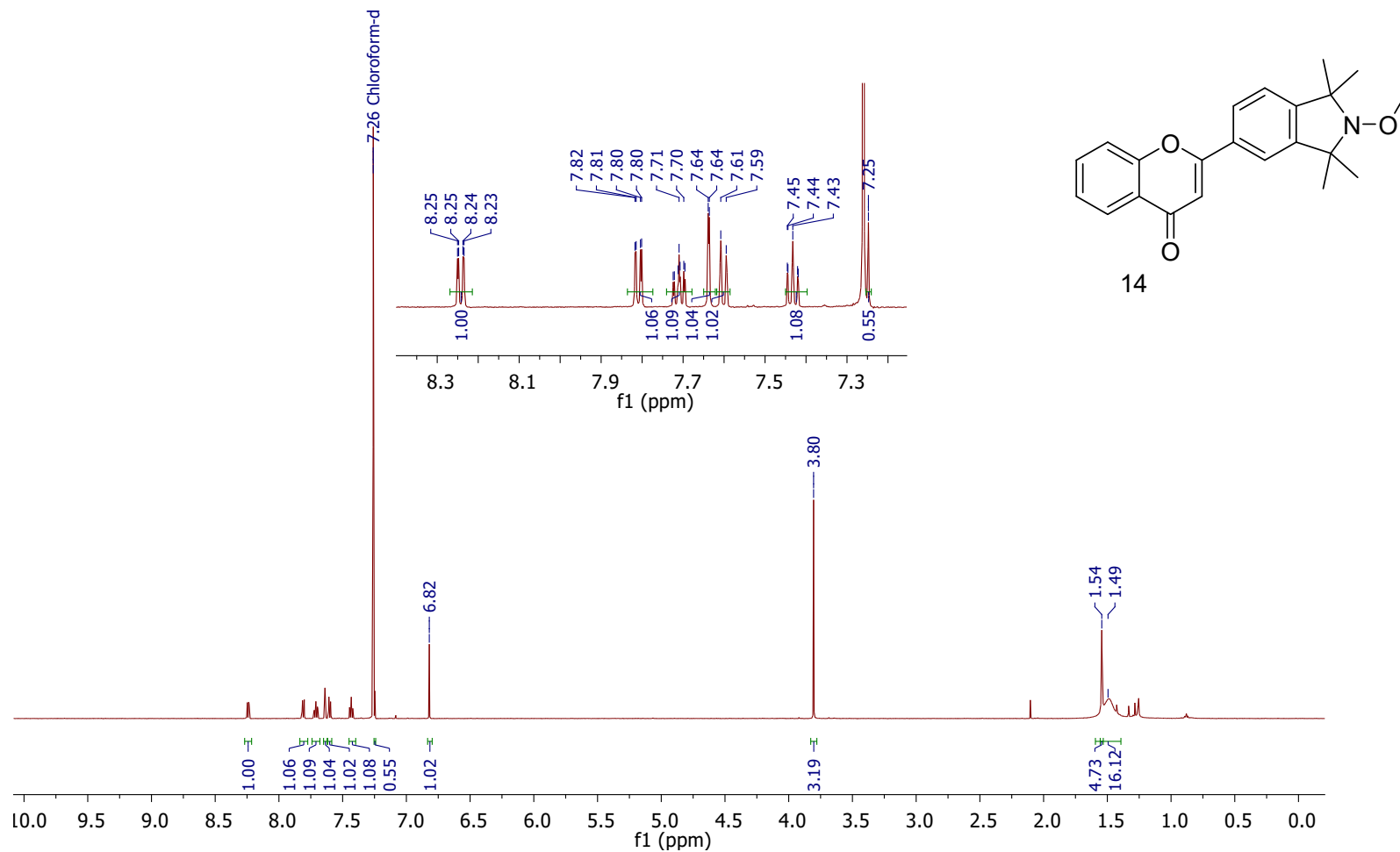


Figure S9: ¹H NMR Spectrum of **14** (CDCl₃, 600 MHz).

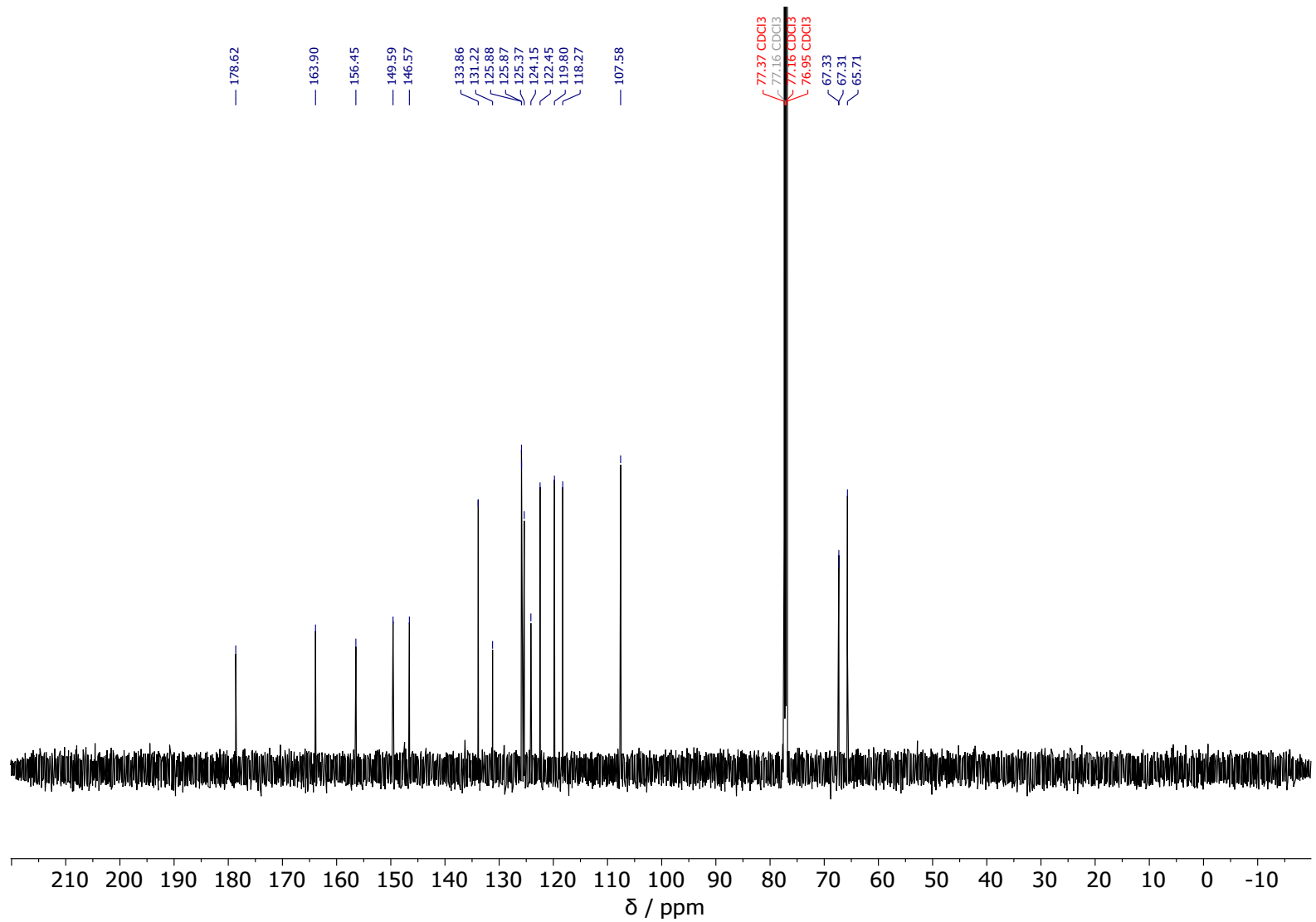


Figure S10: ^{13}C NMR spectrum of **14** (CDCl_3 , 151 MHz).

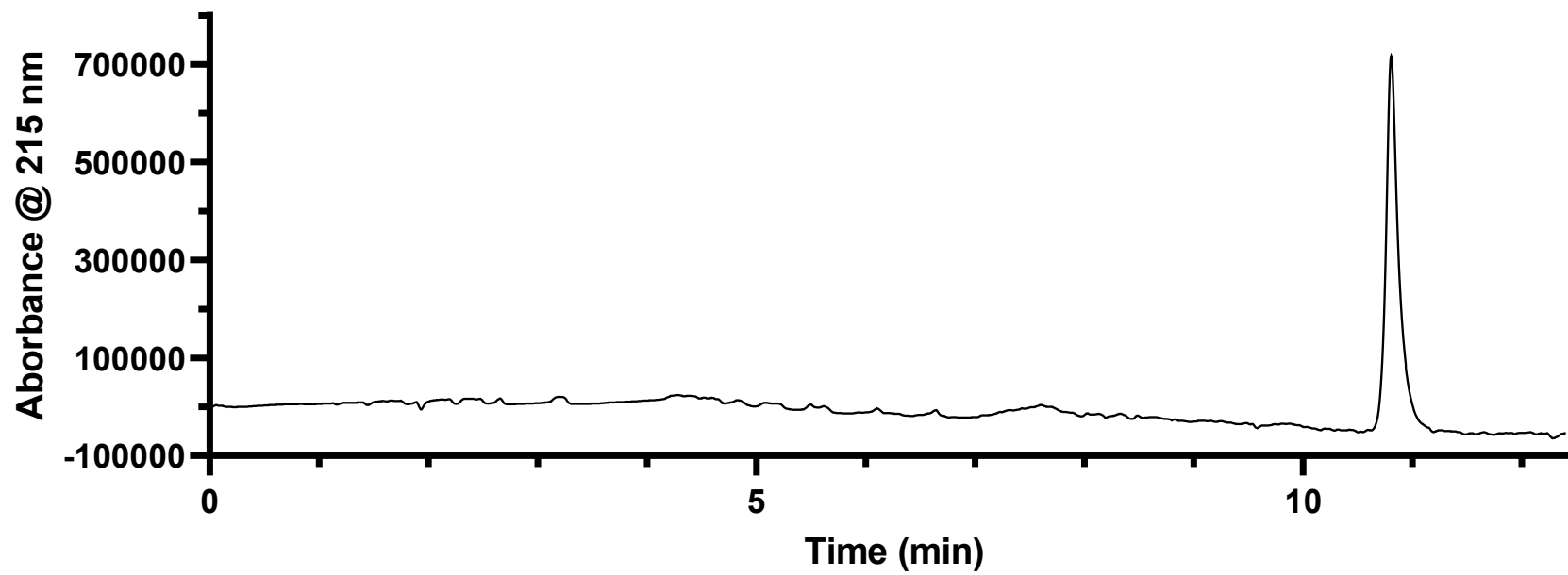


Figure S11: LC trace (215 nm detector wavelength) of **14**. The gradient was altered for this compound to ACN:H₂O (0.1% formic acid) 10:90 – 80:20.

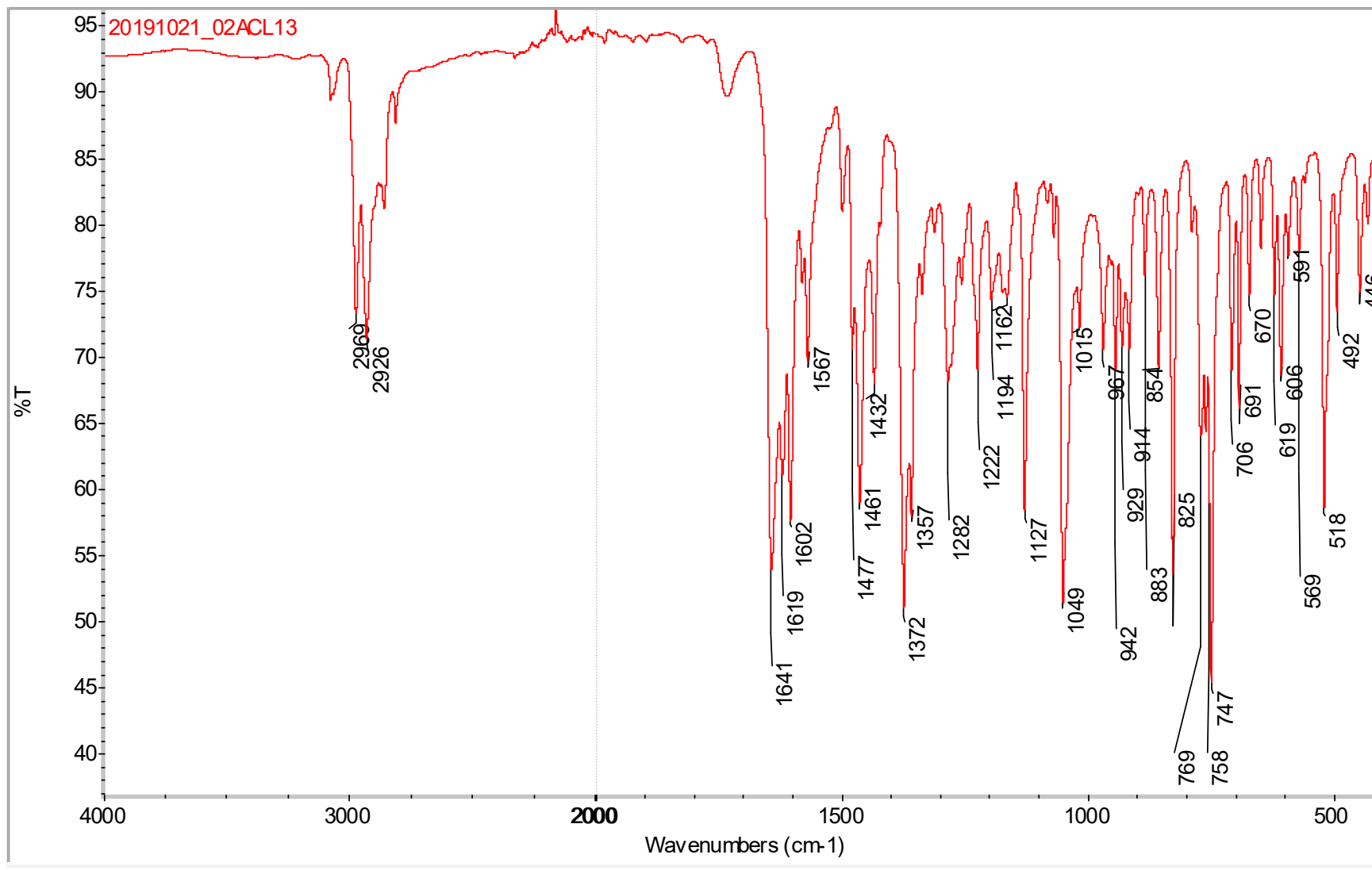


Figure S12: FT-IR spectrum of **14**

2-(2-Methoxy-1,1,3,3-tetramethylisoindolin-5-yl)-3-(2-methoxy-1,1,3,3-tetramethylisoindoline-5-carbonyl)-4H-chromen-4-one (**15**).

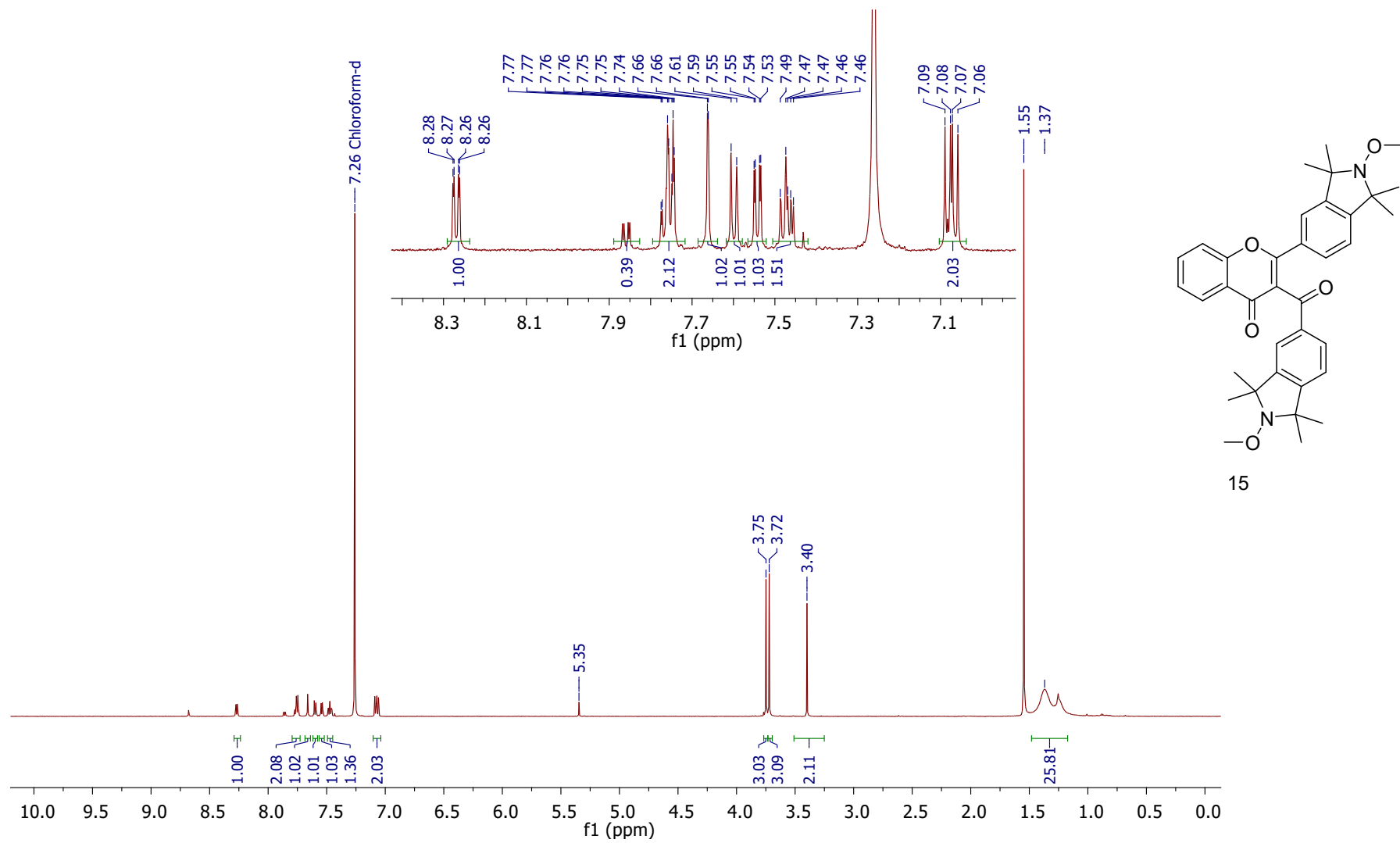


Figure S13: ¹H NMR spectrum of **15** (CDCl₃, 600 MHz).

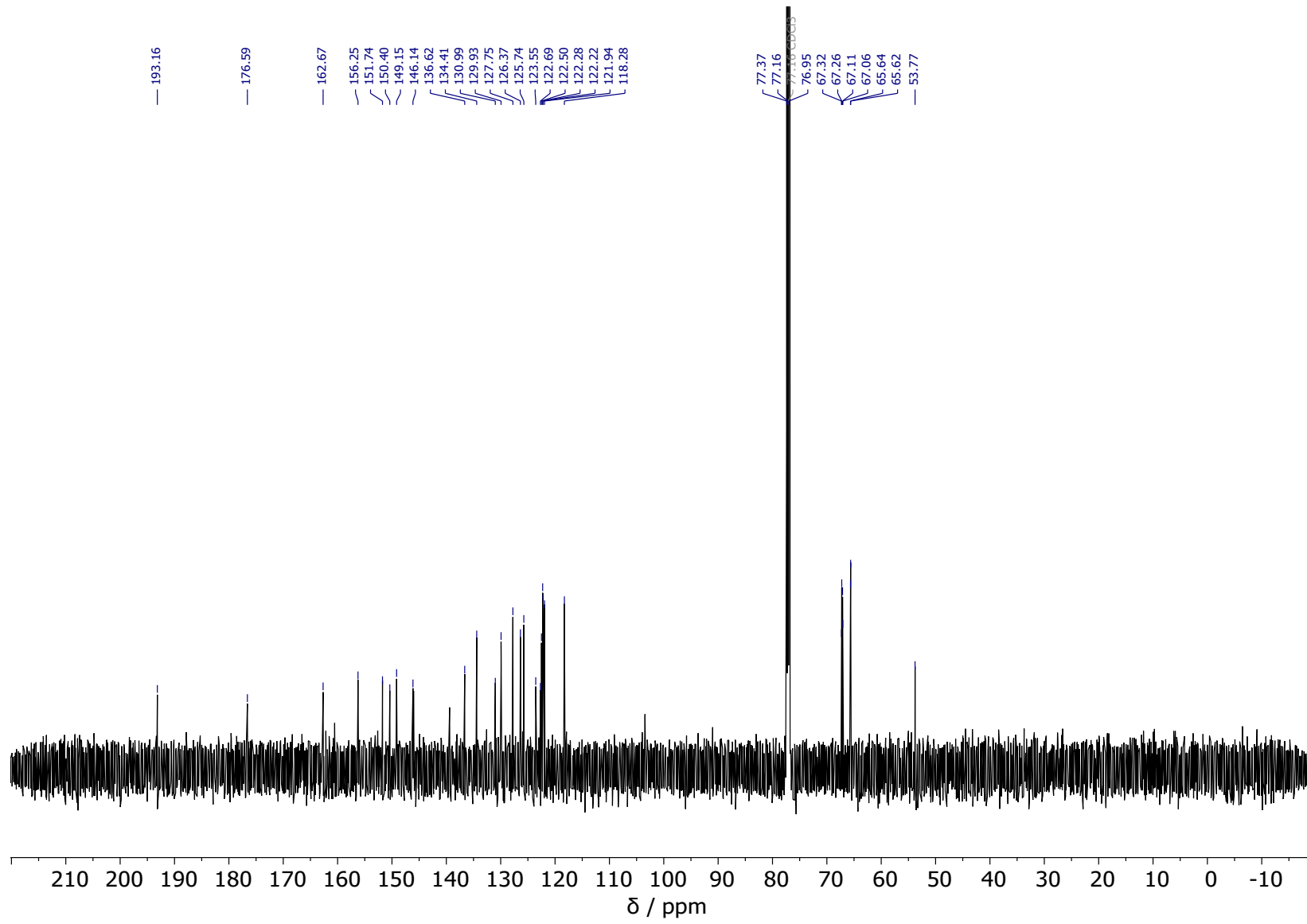


Figure S14: ^{13}C NMR spectrum of **15** (CDCl₃, 151 MHz).

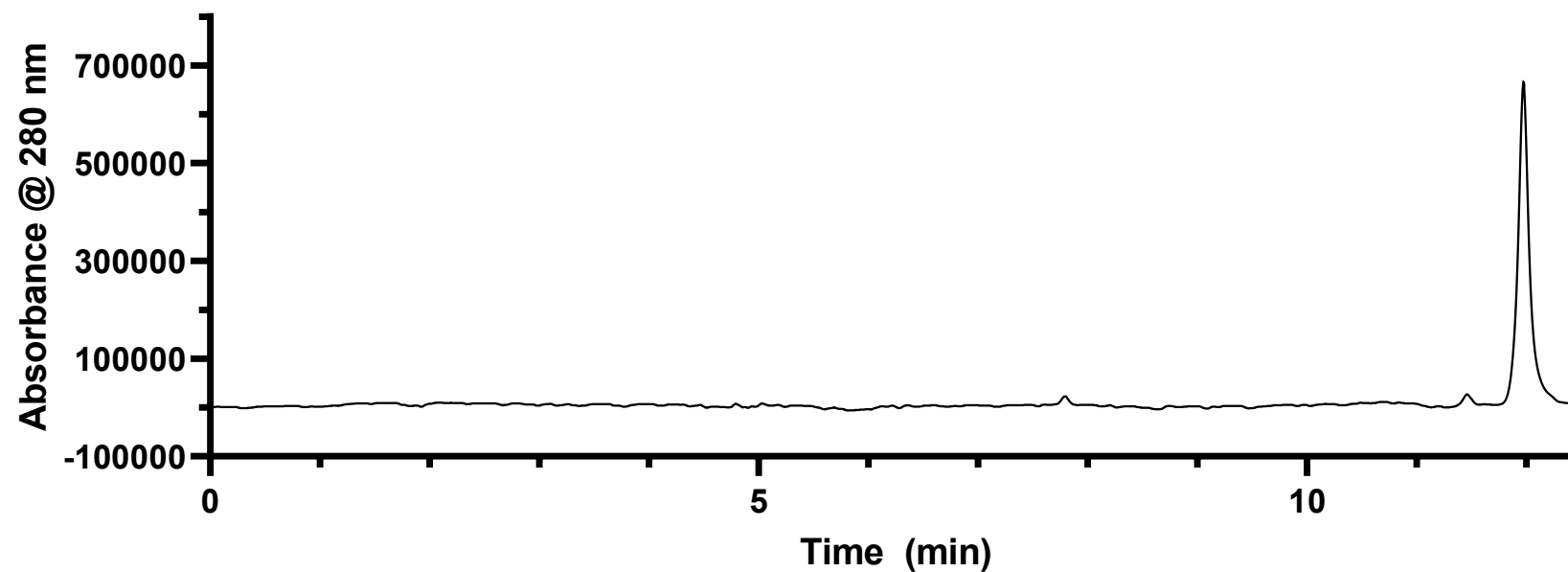


Figure S15: LC trace (280 nm detector wavelength) of **15**. The gradient was altered for this compound to ACN:H₂O (0.1% formic acid) 10:90 – 80:20.

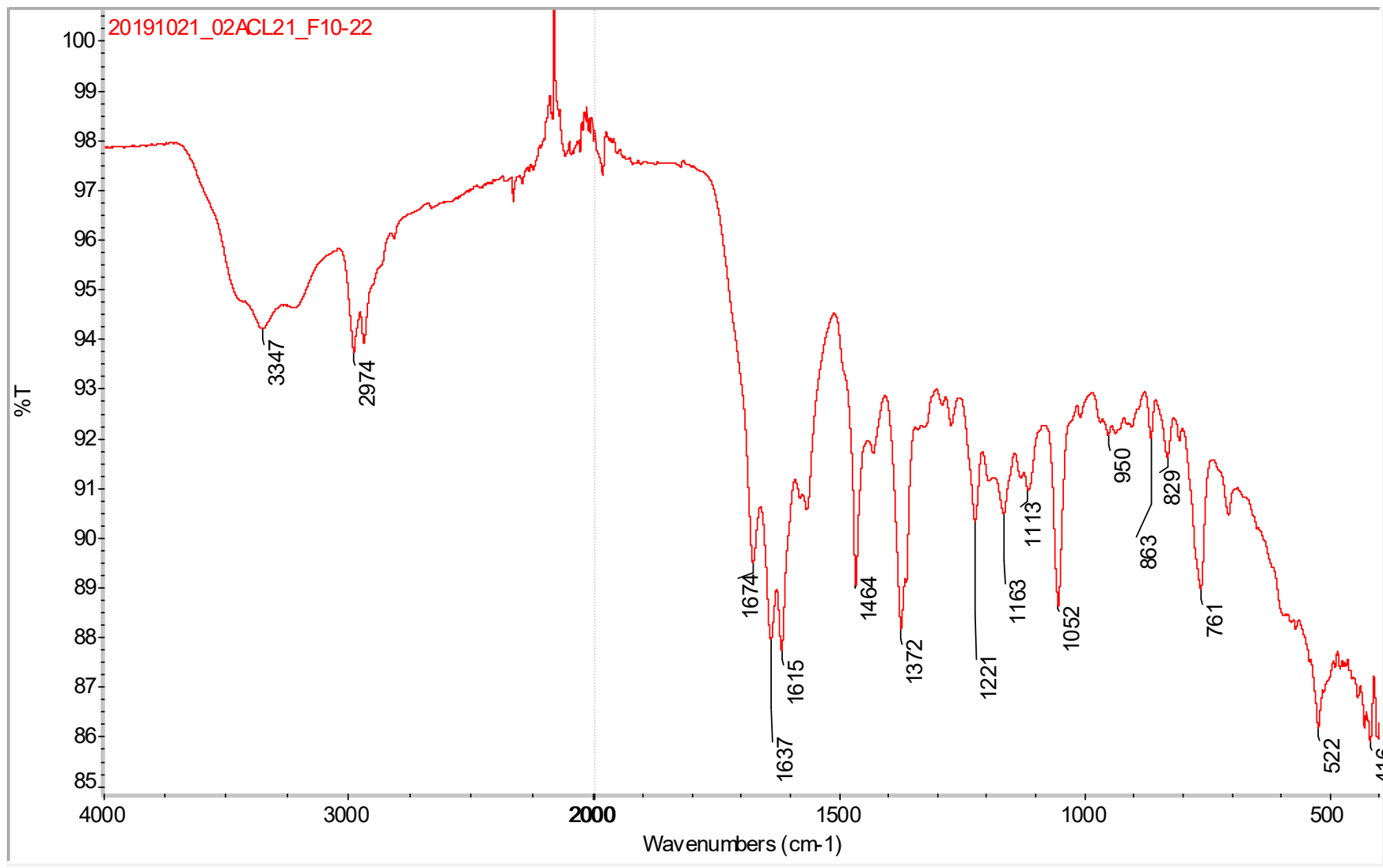


Figure S16: FT-IR spectrum of **15**

2-(1,1,3,3-Tetramethylisoindolin-2-oxyl)-4H-chromen-4-one (6)

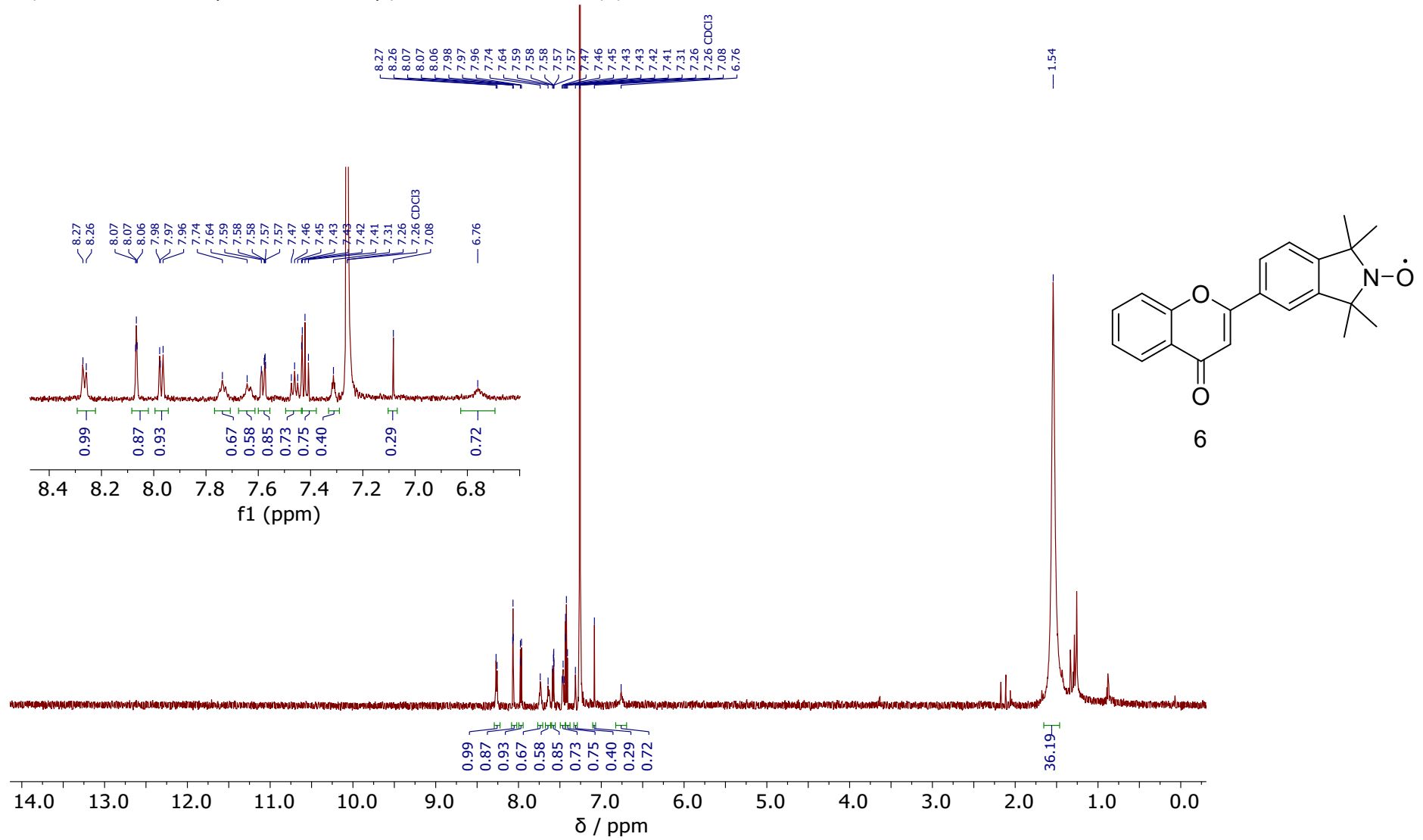


Figure S17: ^1H NMR spectrum of **6** (CDCl_3 , 600 MHz). Note: Nitroxide radicals often cause broad NMR signals, inaccurate integration, and missing integrals.

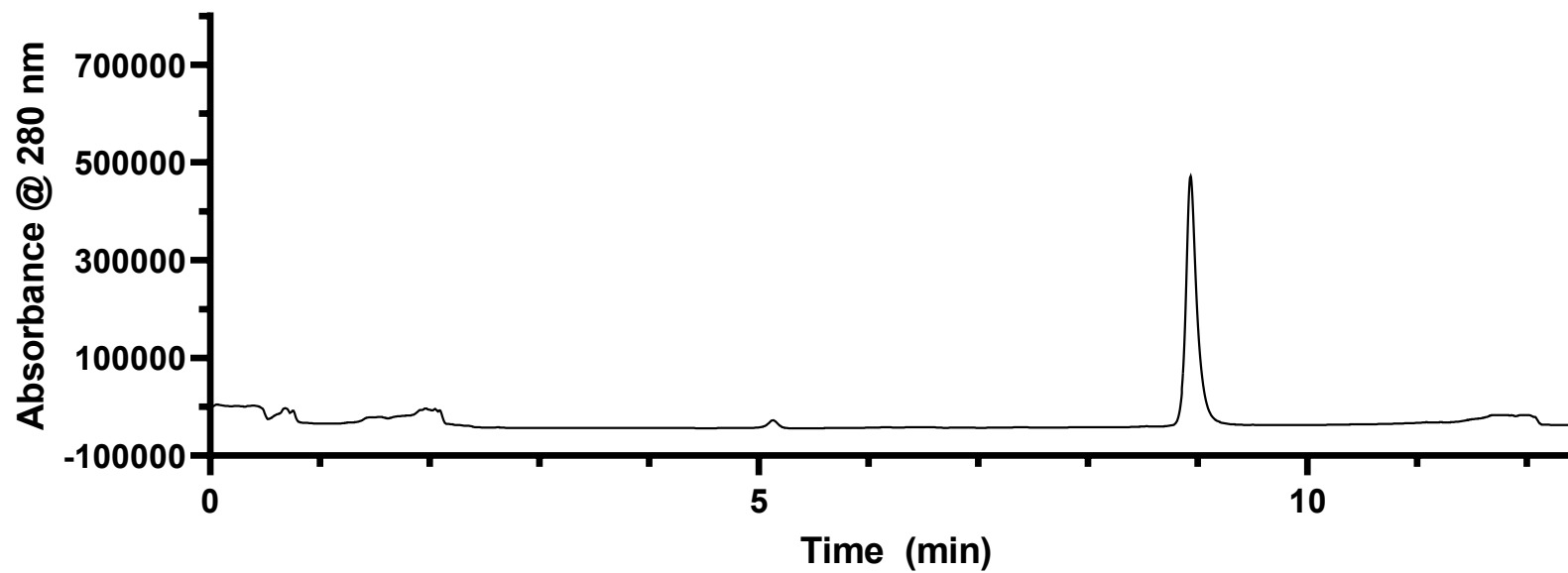


Figure S18: LC trace (280 nm detector wavelength) of **6**. The gradient was altered for this compound to ACN:H₂O (0.1% formic acid) 10:90 – 80:20.

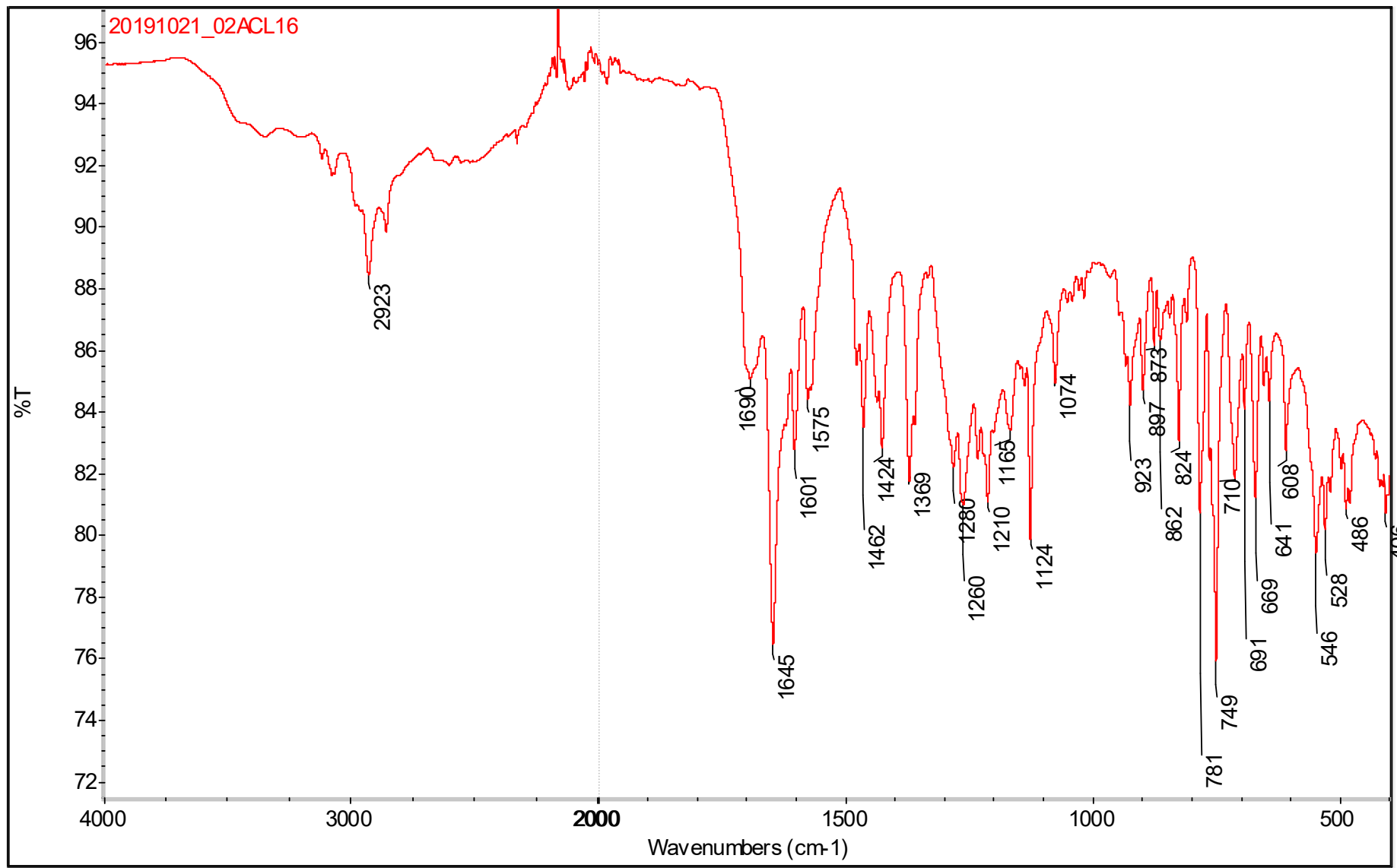


Figure S19: FT-IR spectra of **6**.

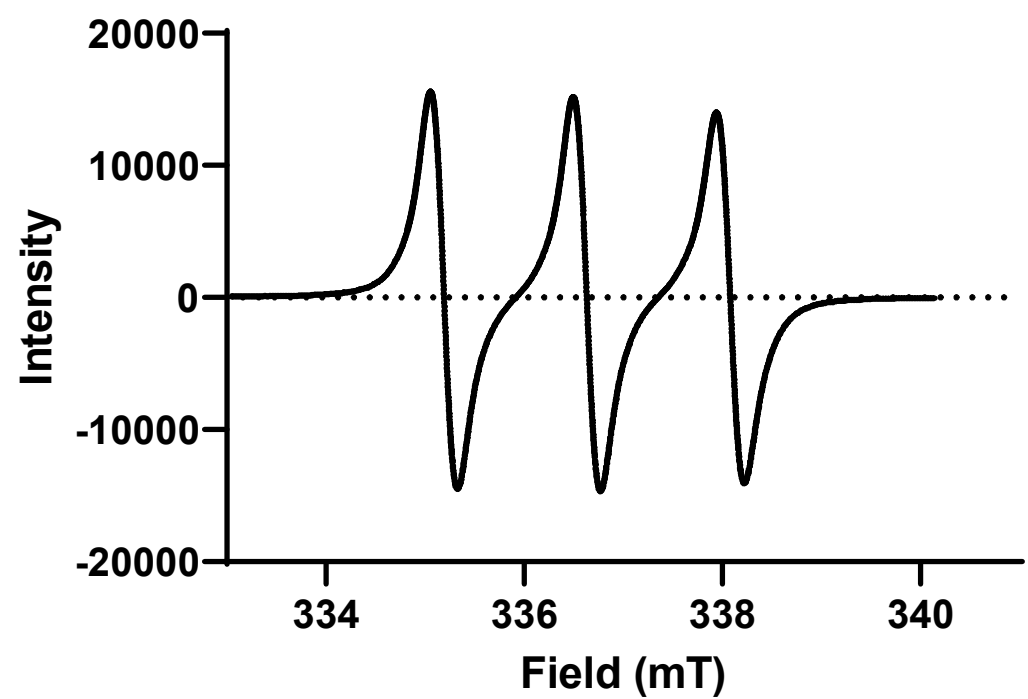


Figure S20: EPR spectrum of **6** in CDCl_3 ($a_n = 1.44 \text{ mT}$, $T = 298 \text{ K}$)

2-(1,1,3,3-Tetramethylisoindolin-2-oxyl)-3-(1,1,3,3-tetramethylisoindolin-2-oxyl-5-carbonyl)-4H-chromen-4-one (**8**)

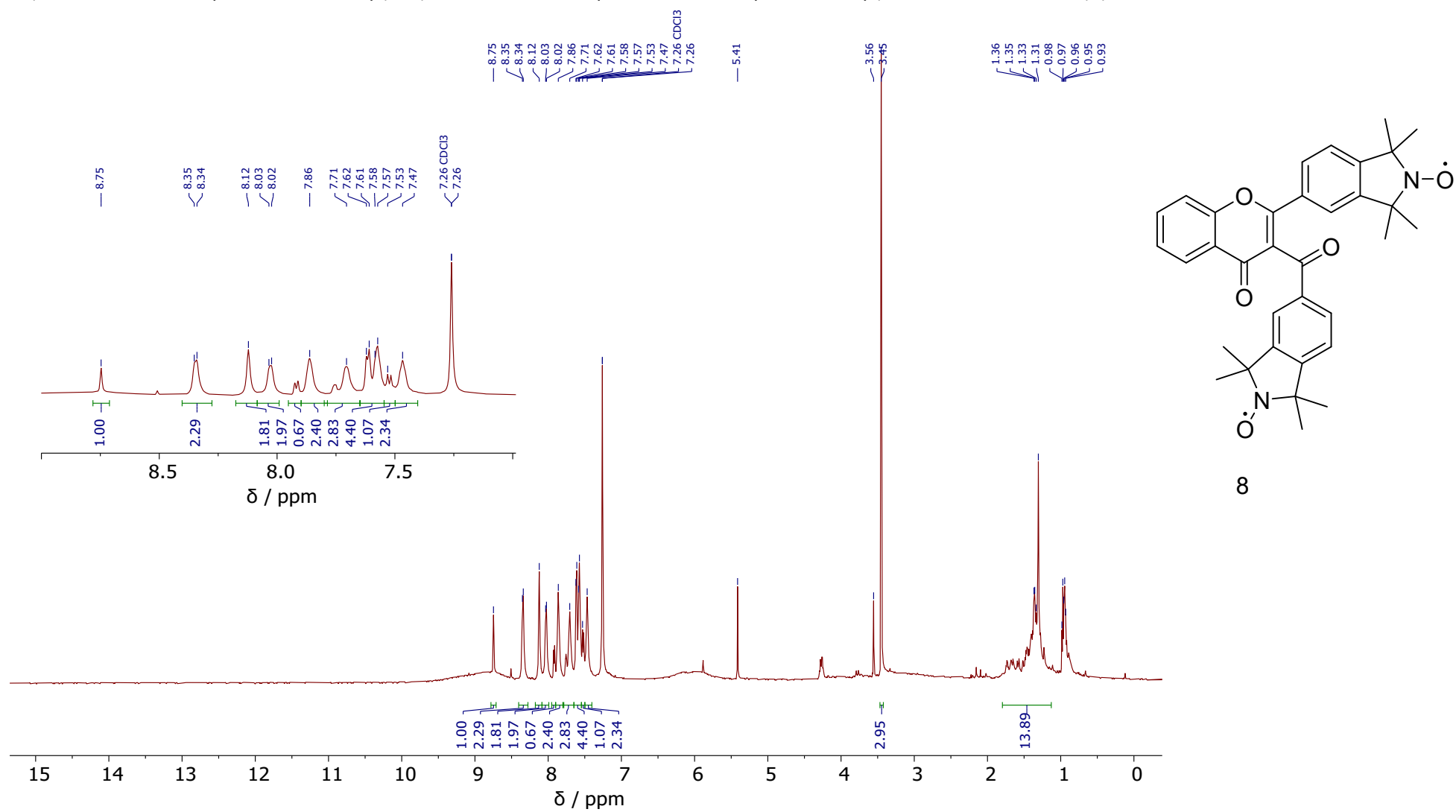


Figure S21: ^1H NMR Spectrum of **8** (CDCl_3 , 600 MHz). Note: Nitroxide radicals often cause broad NMR signals, inaccurate integration, and missing integrals.

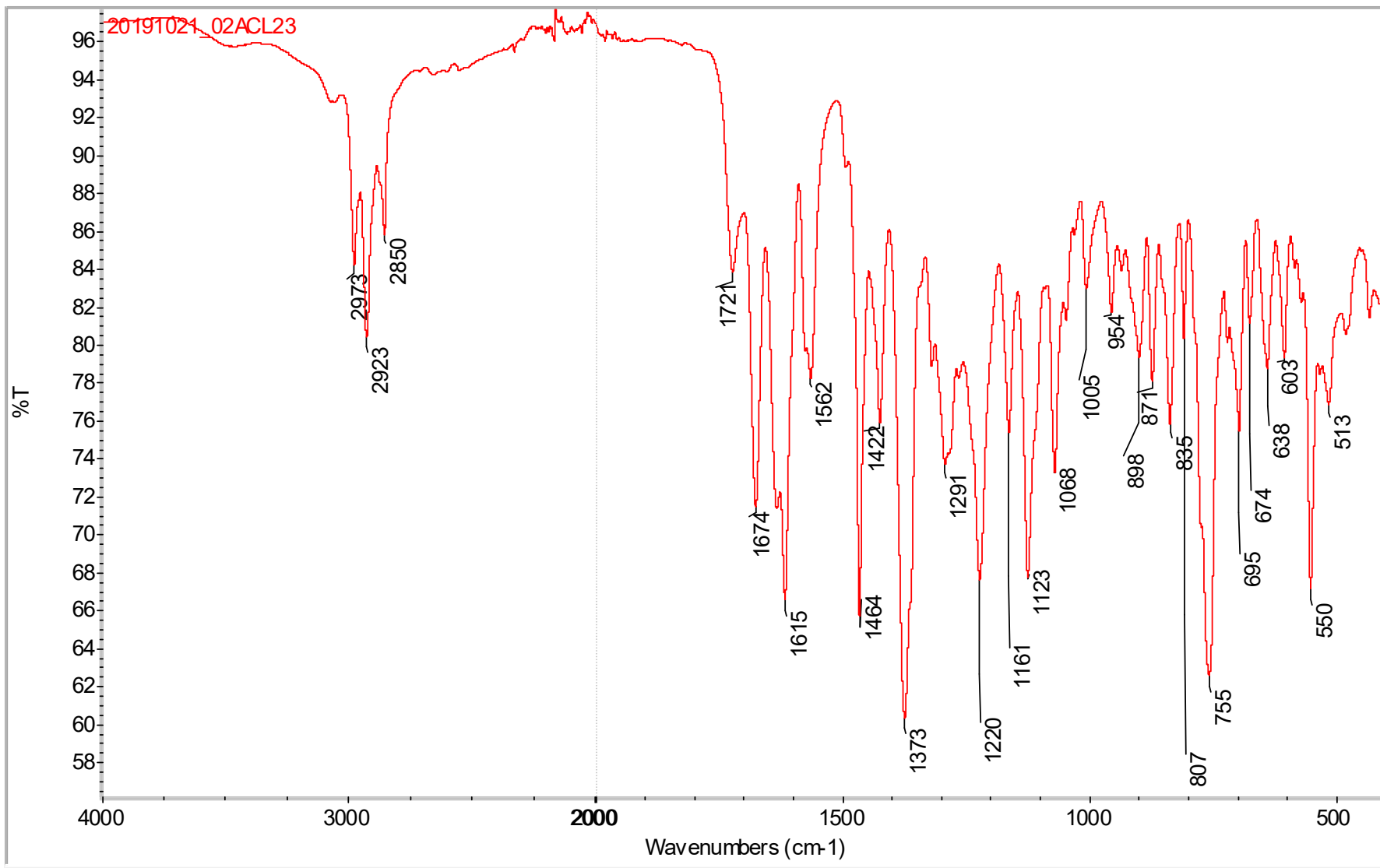


Figure S22: FT-IR spectrum of **8**.

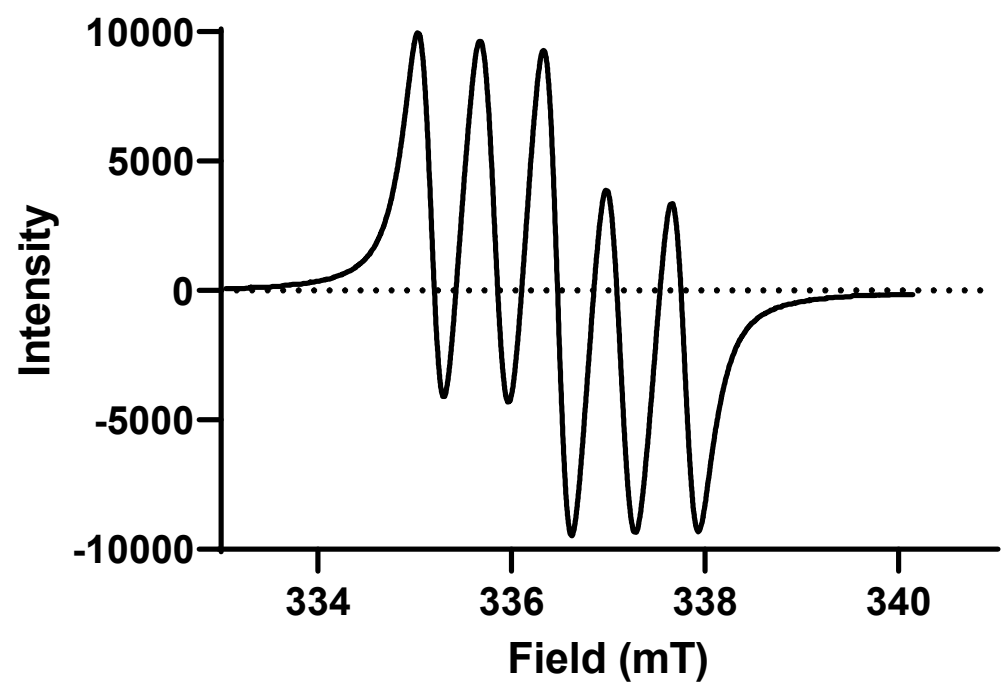


Figure S23: EPR Spectrum of **8** in CDCl_3 ($a_N = 1.294$ mT, $T = 298$ K).

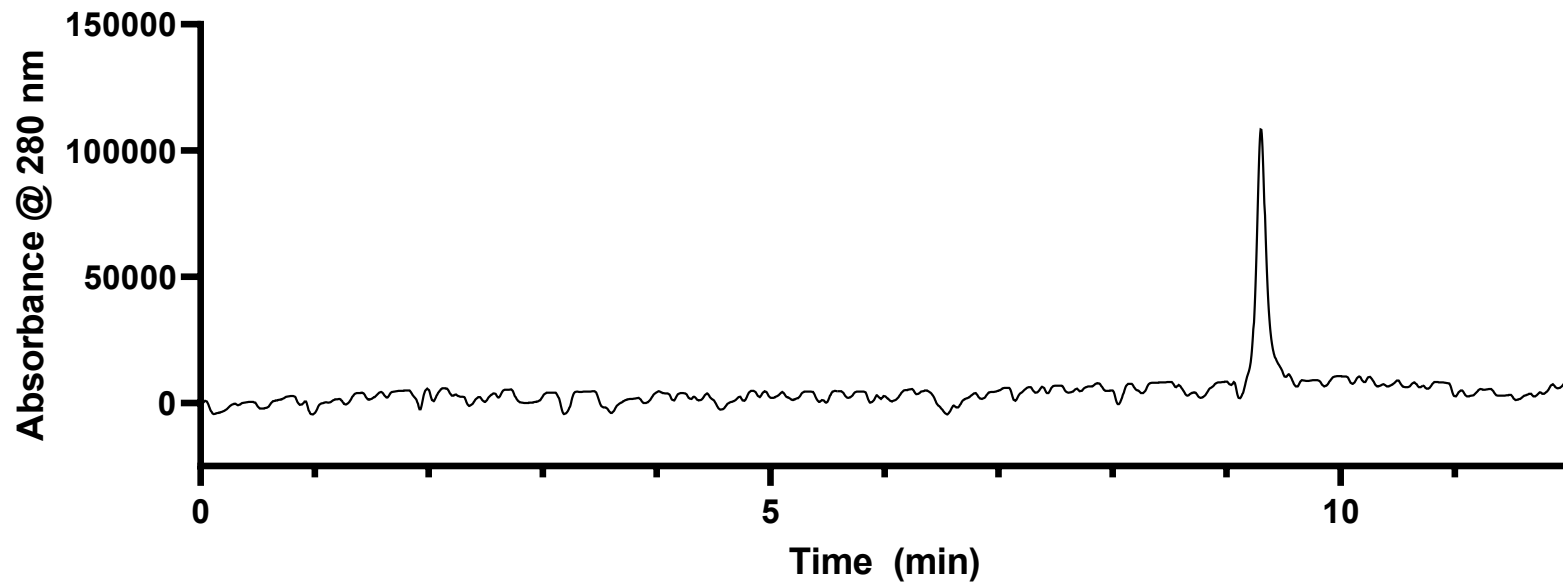


Figure S24: LC trace (280 nm detector wavelength) of **8**. The gradient was altered for this compound to ACN:H₂O (0.1% formic acid) 10:90 – 80:20.

2-Acetyl-3-hydroxyphenyl 2-methoxy-1,1,3,3-tetramethylisoindoline-5-carboxylate (17)

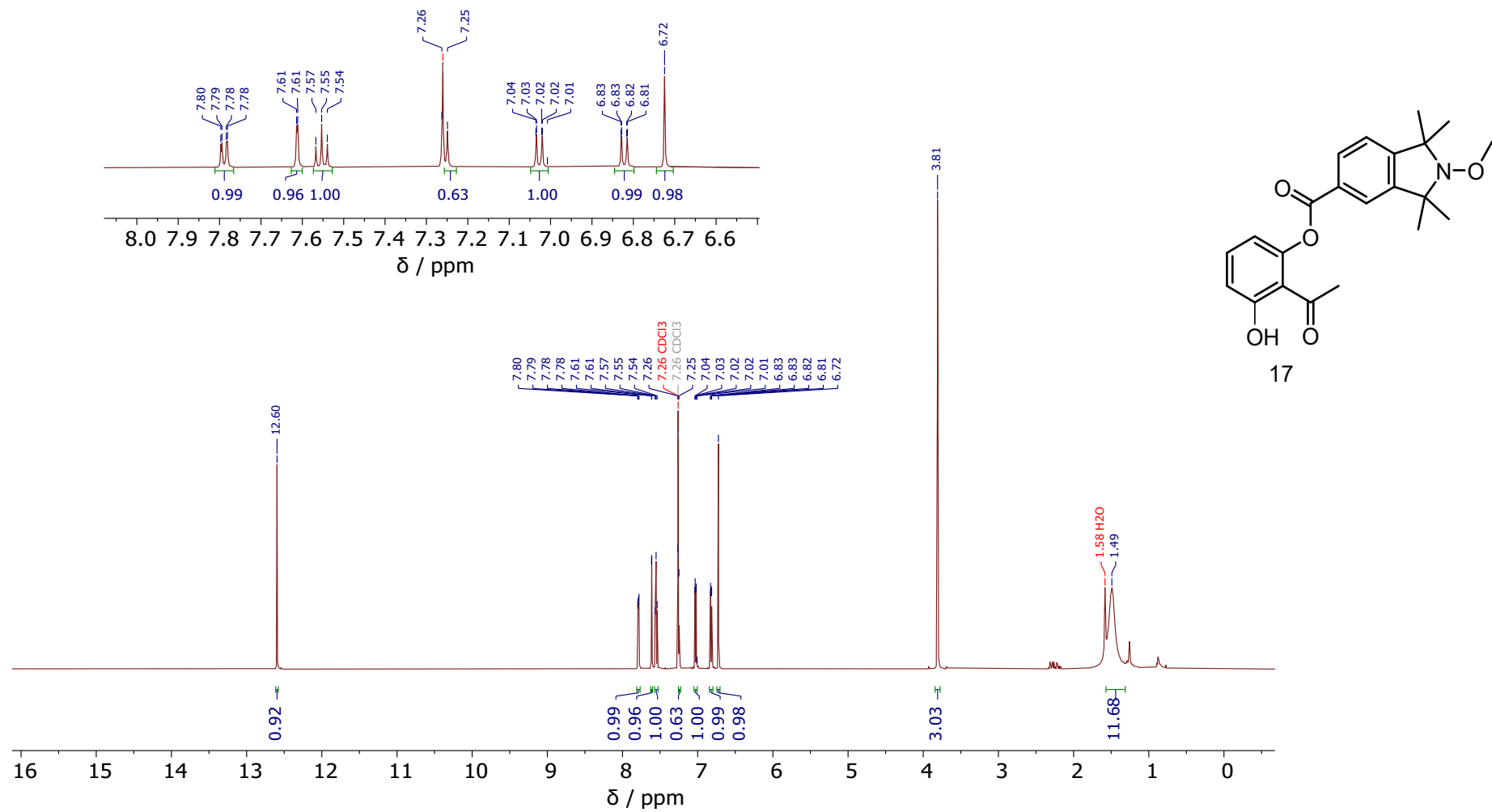


Figure S25: ^1H NMR spectrum of **17** (CDCl₃, 600 MHz).

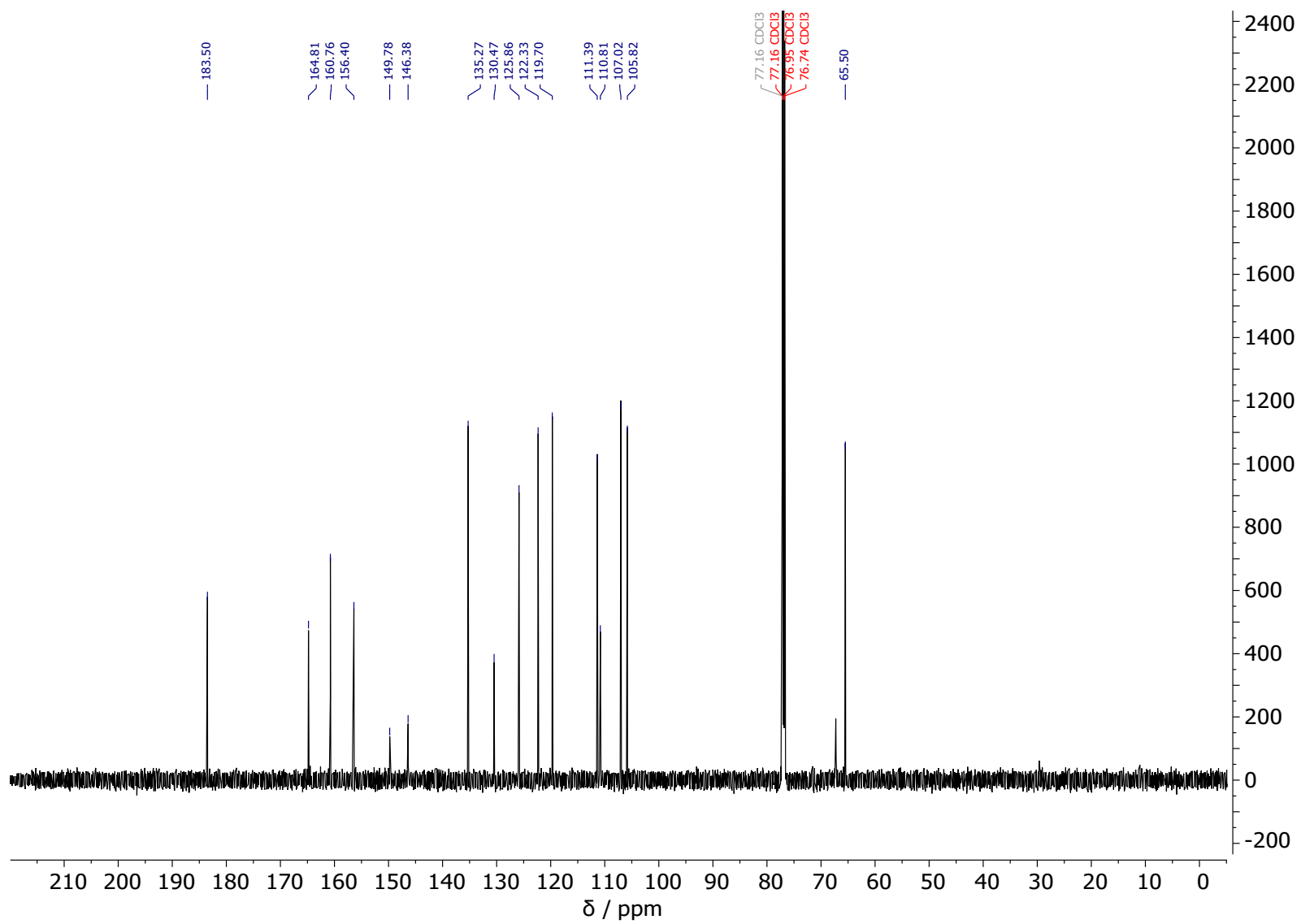


Figure S26: ^{13}C NMR spectrum of **17** (CDCl₃, 151 MHz).

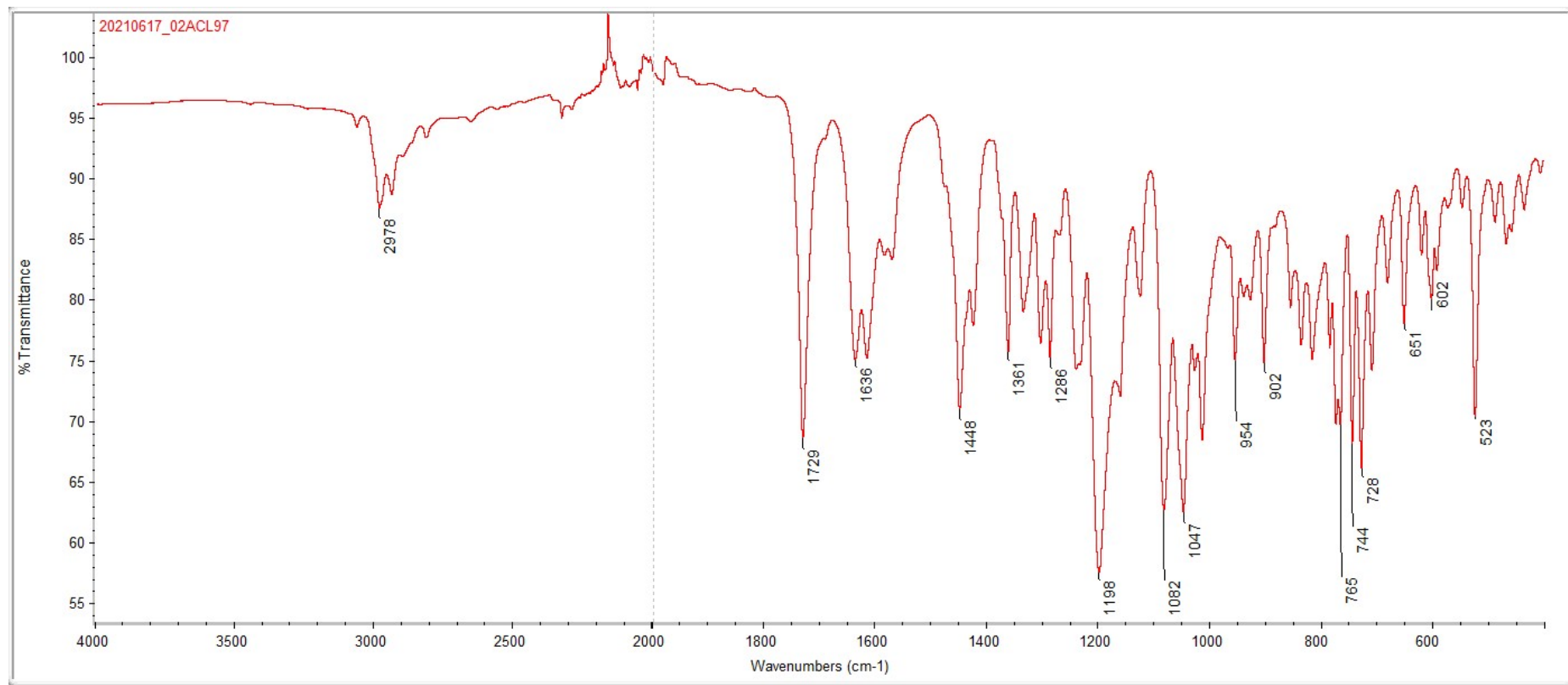


Figure S27: FT-IR spectrum of **17**

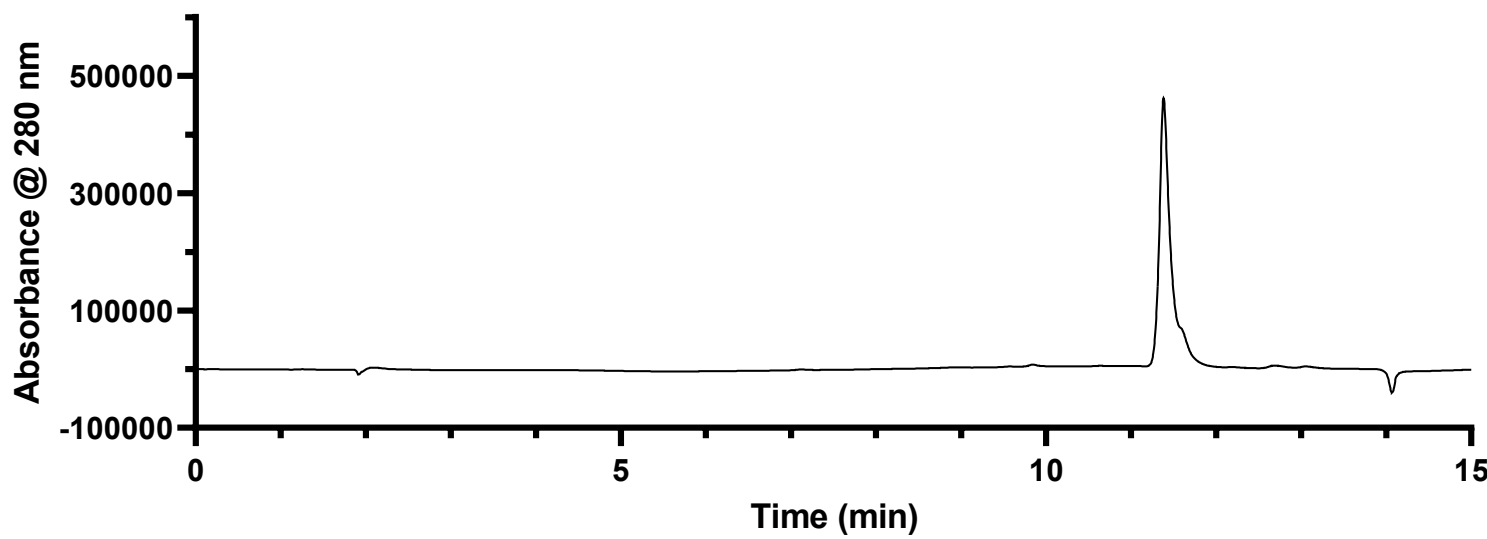


Figure S28: LC trace (280 nm detector wavelength) of **17**. The gradient was altered for this compound to ACN:H₂O (0.1% formic acid) 10:90 – 80:20.

5-Hydroxy-2-(2-methoxy-1,1,3,3-tetramethylisoindolin-5-yl)-4H-chromen-4-one (**18**)

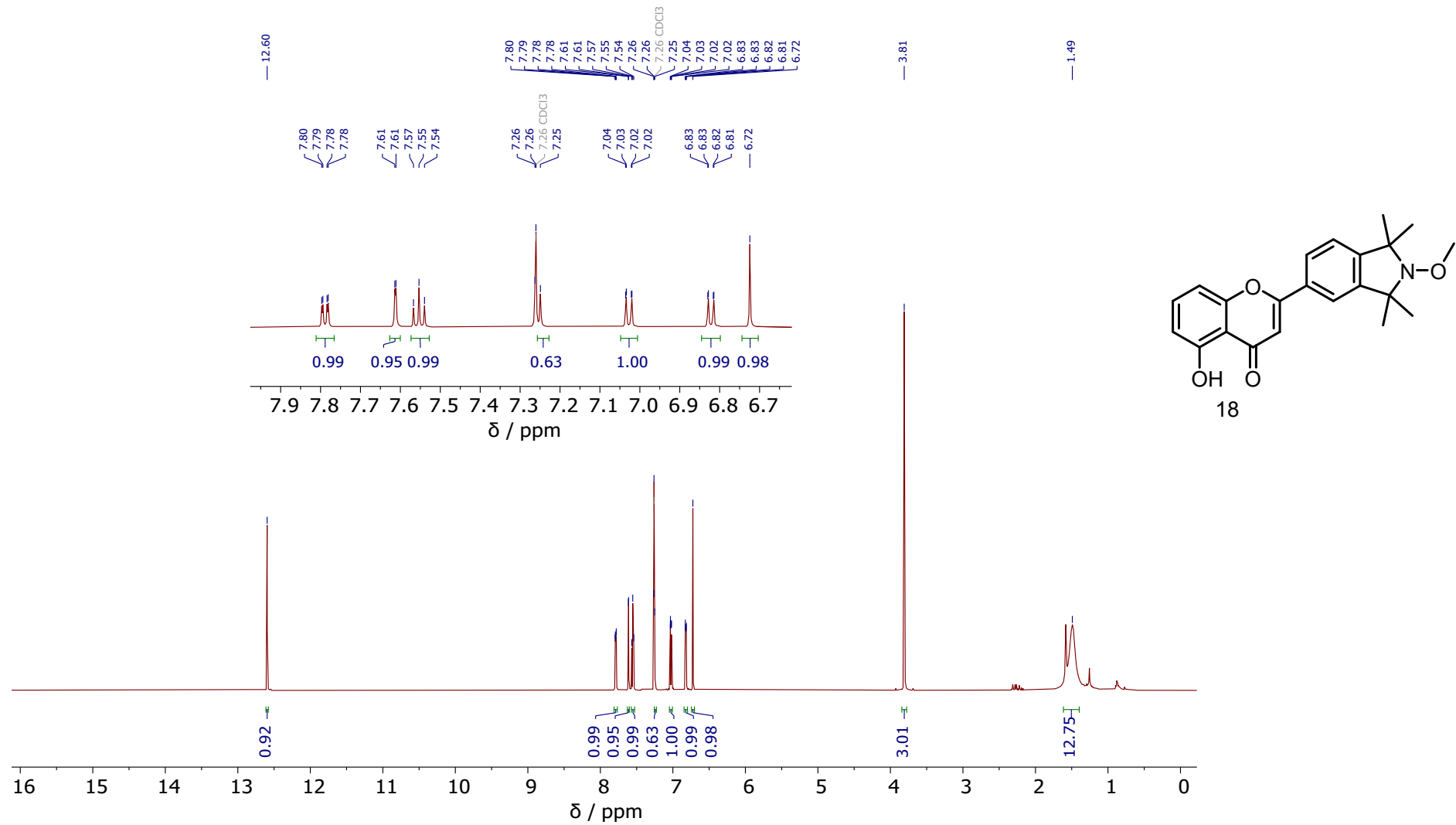


Figure S33: ^1H NMR spectrum of **18** (CDCl_3 , 600 MHz).

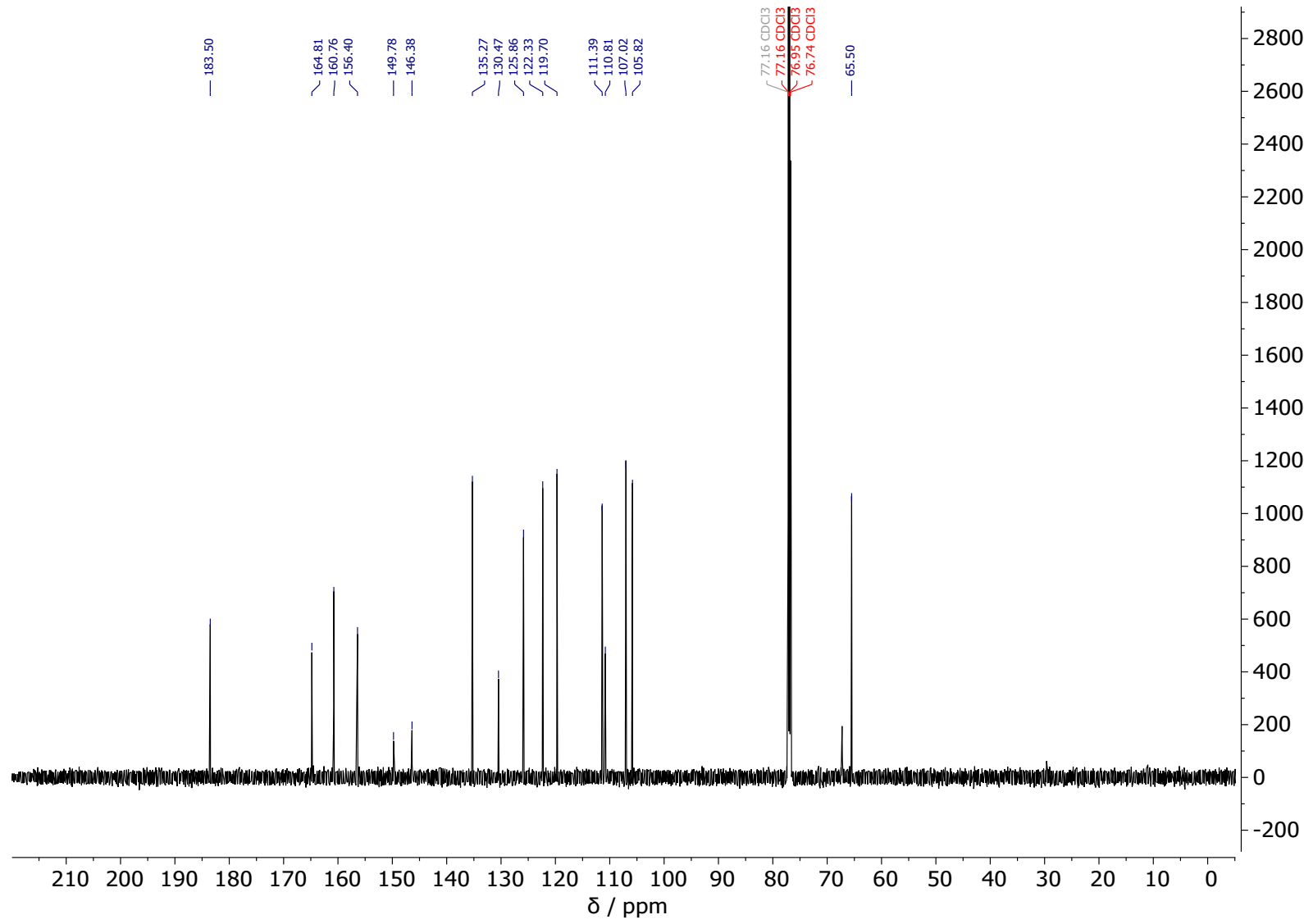


Figure S34: ^{13}C NMR spectrum of **18** (CDCl₃, 151 MHz).

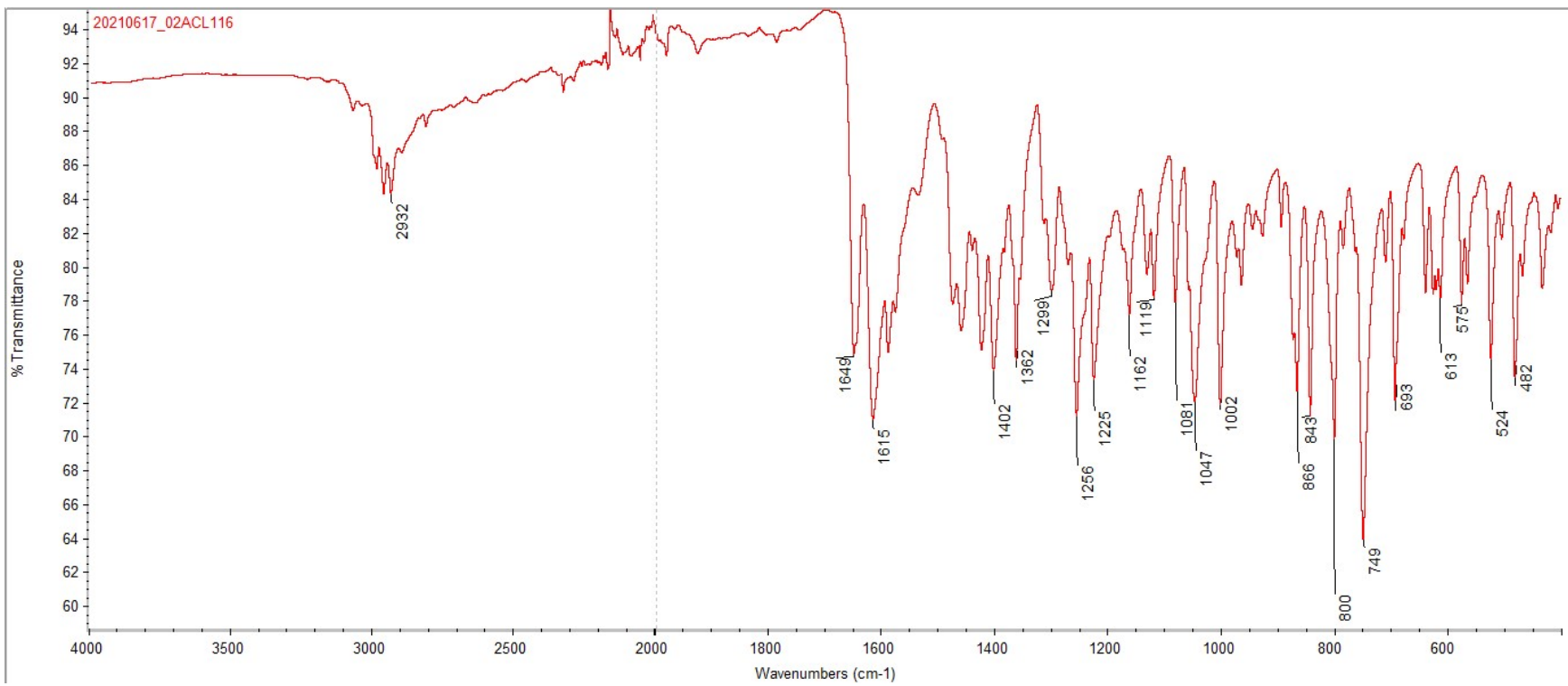


Figure S35: FT-IR Spectrum of **18**

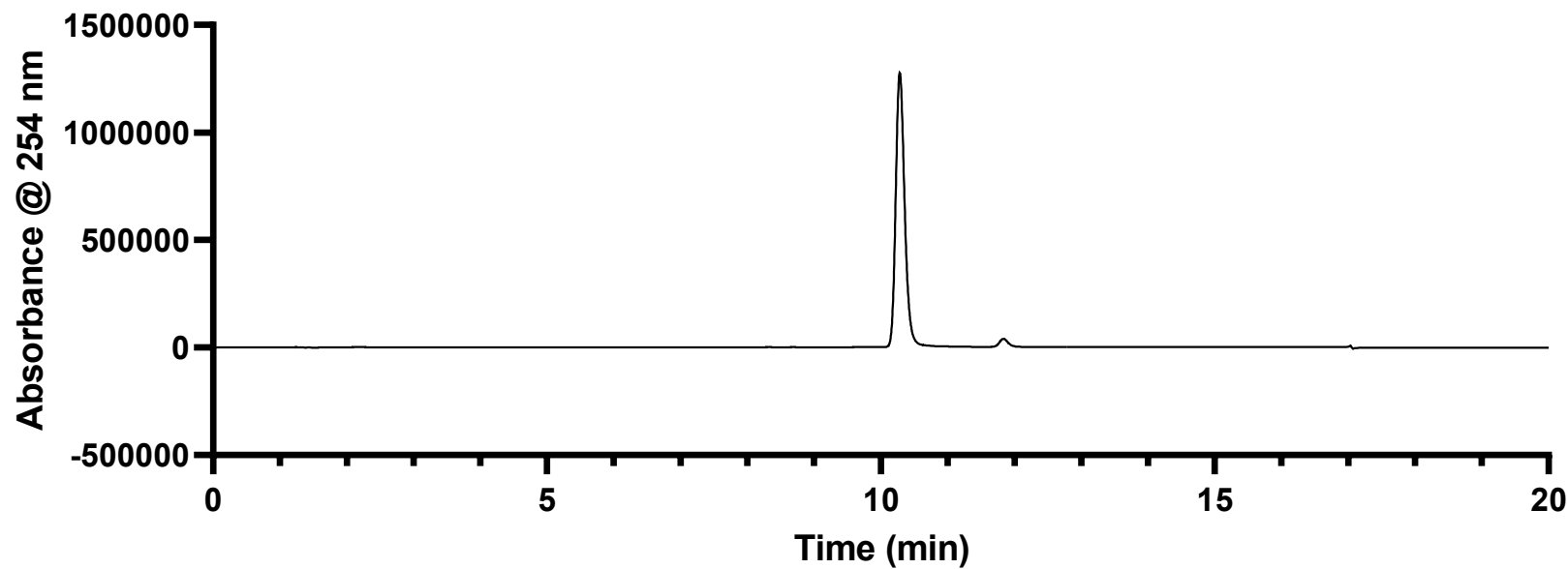


Figure S36: LC trace (254 nm detector wavelength) of **18**. The gradient was altered for this compound to ACN:H₂O (0.1% formic acid) 10:90 – 80:20.

2-Acetyl-1,3-phenylene bis(2-methoxy-1,1,3,3-tetramethylisoindoline-5-carboxylate) (**19**)

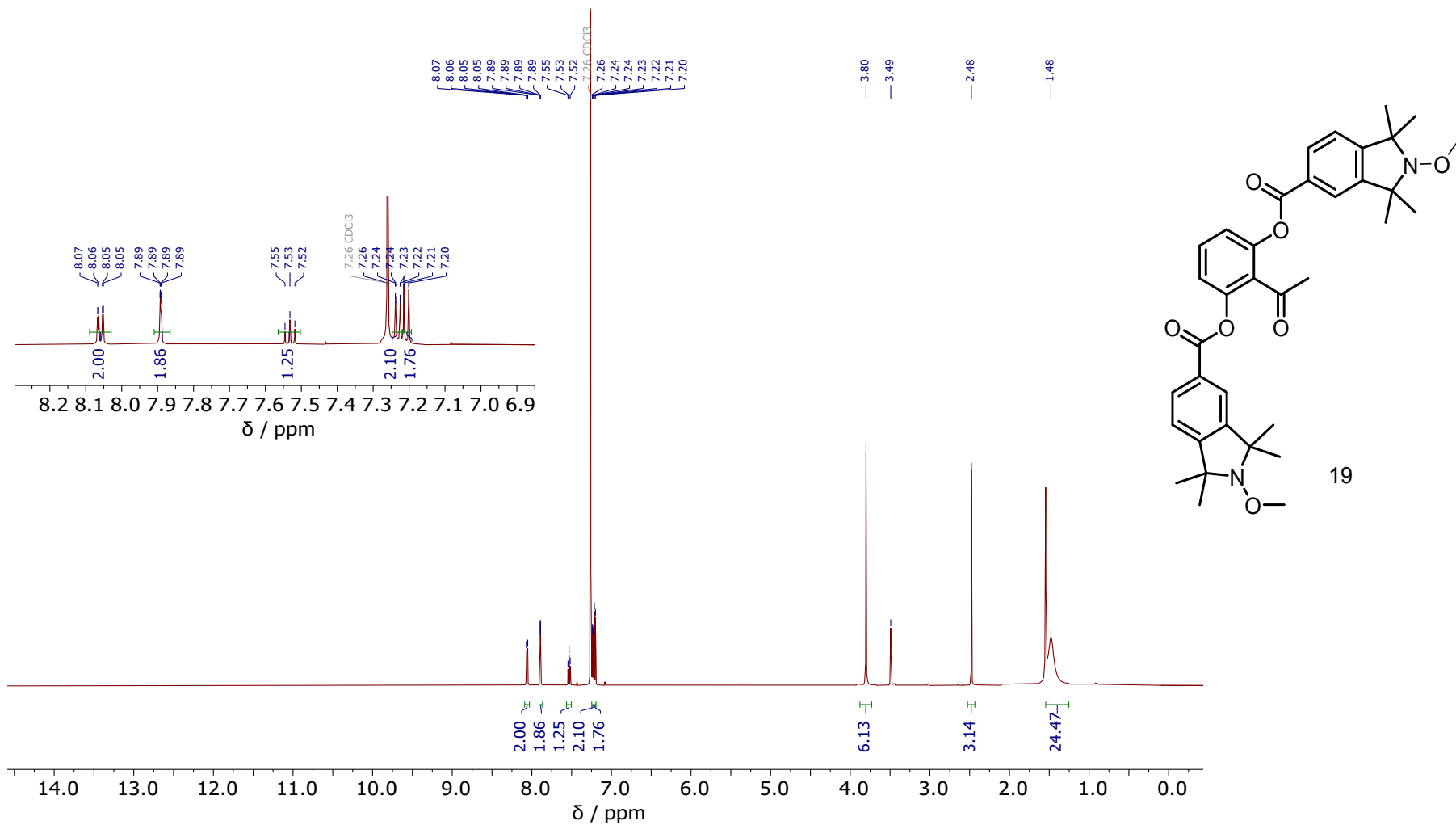


Figure S29: ¹H NMR spectrum of **19** (CDCl₃, 600 MHz).

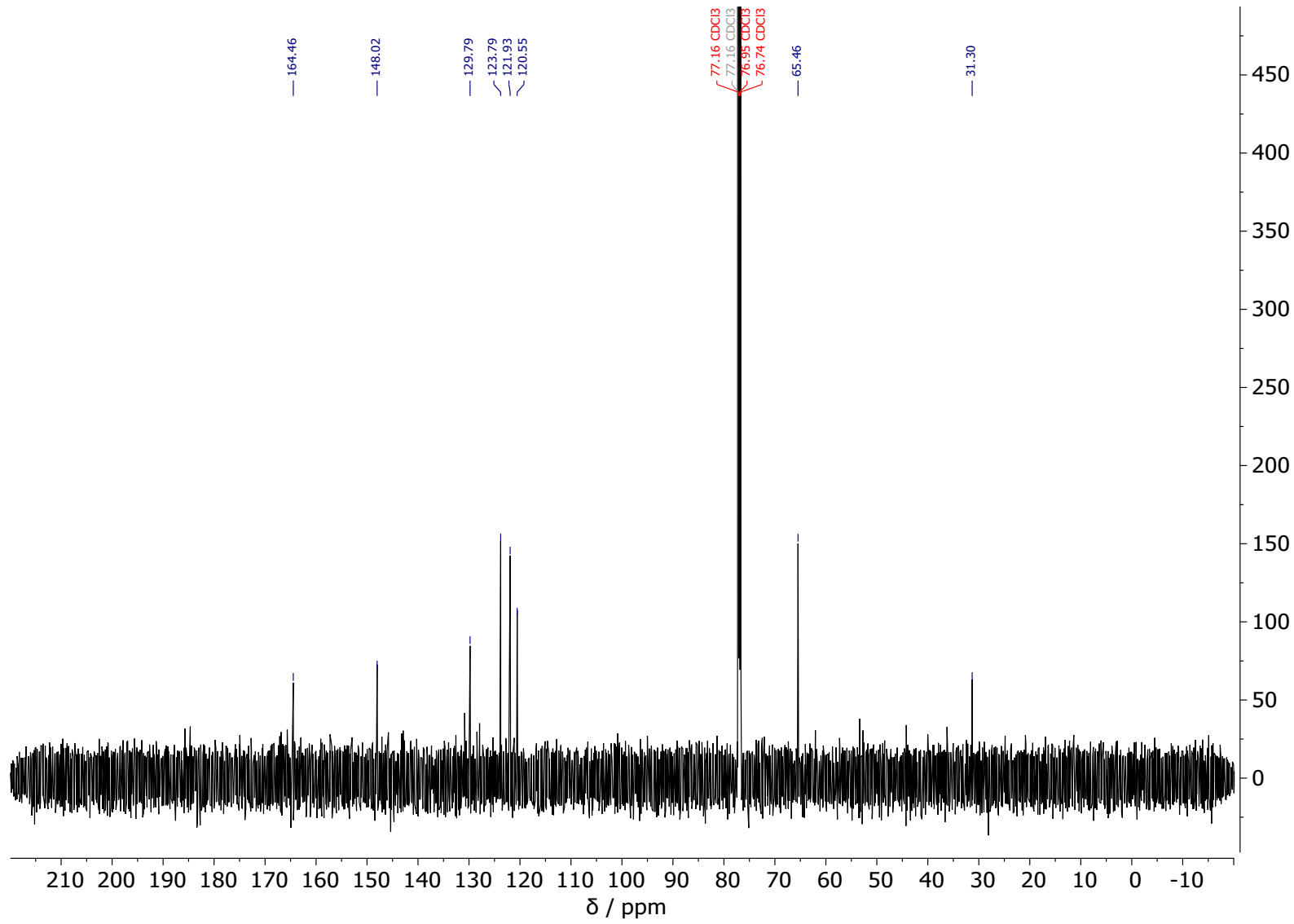


Figure S30: ^{13}C NMR spectrum of **19** (CDCl₃, 151 MHz).

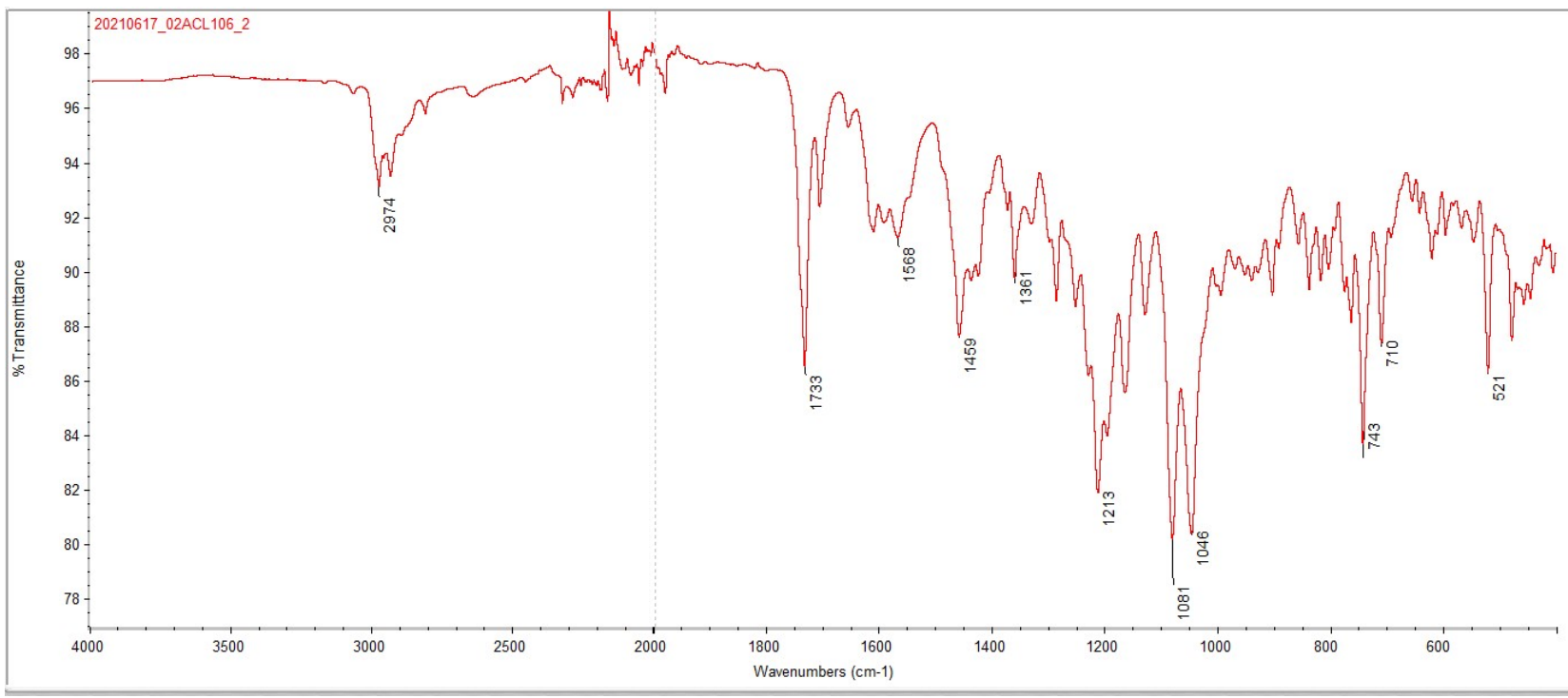


Figure S31: FT-IR spectrum of **19**.

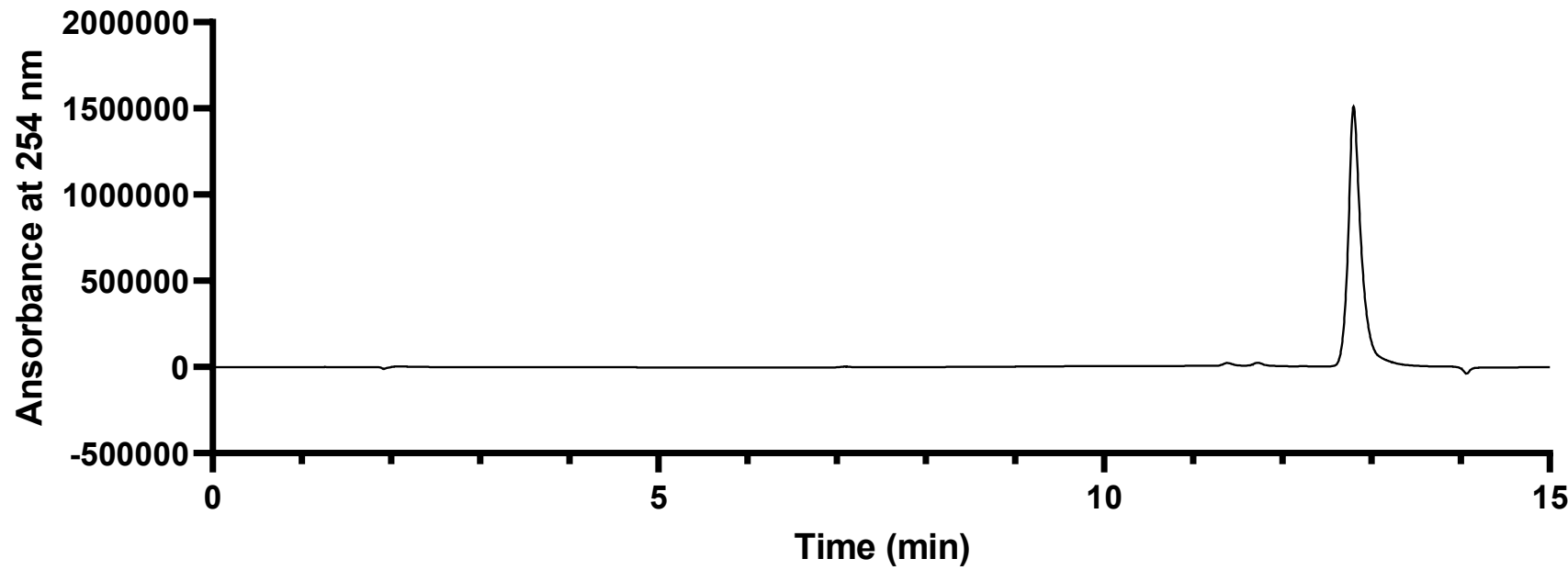


Figure S32: LC trace (254 nm detector wavelength) of **19**. The gradient was altered for this compound to ACN:H₂O (0.1% formic acid) 10:90 – 80:20.

5-Hydroxy-2-(2-methoxy-1,1,3,3-tetramethylisoindolin-5-yl)-3-(2-methoxy-1,1,3,3-tetramethylisoindoline-5-carbonyl)-4H-chromen-4-one (20)

20210107_02ACL108.90.fid

02ACL108_F18-25

PROTONRO CDCl₃ {C:\Data\Chemists} AstridL 1

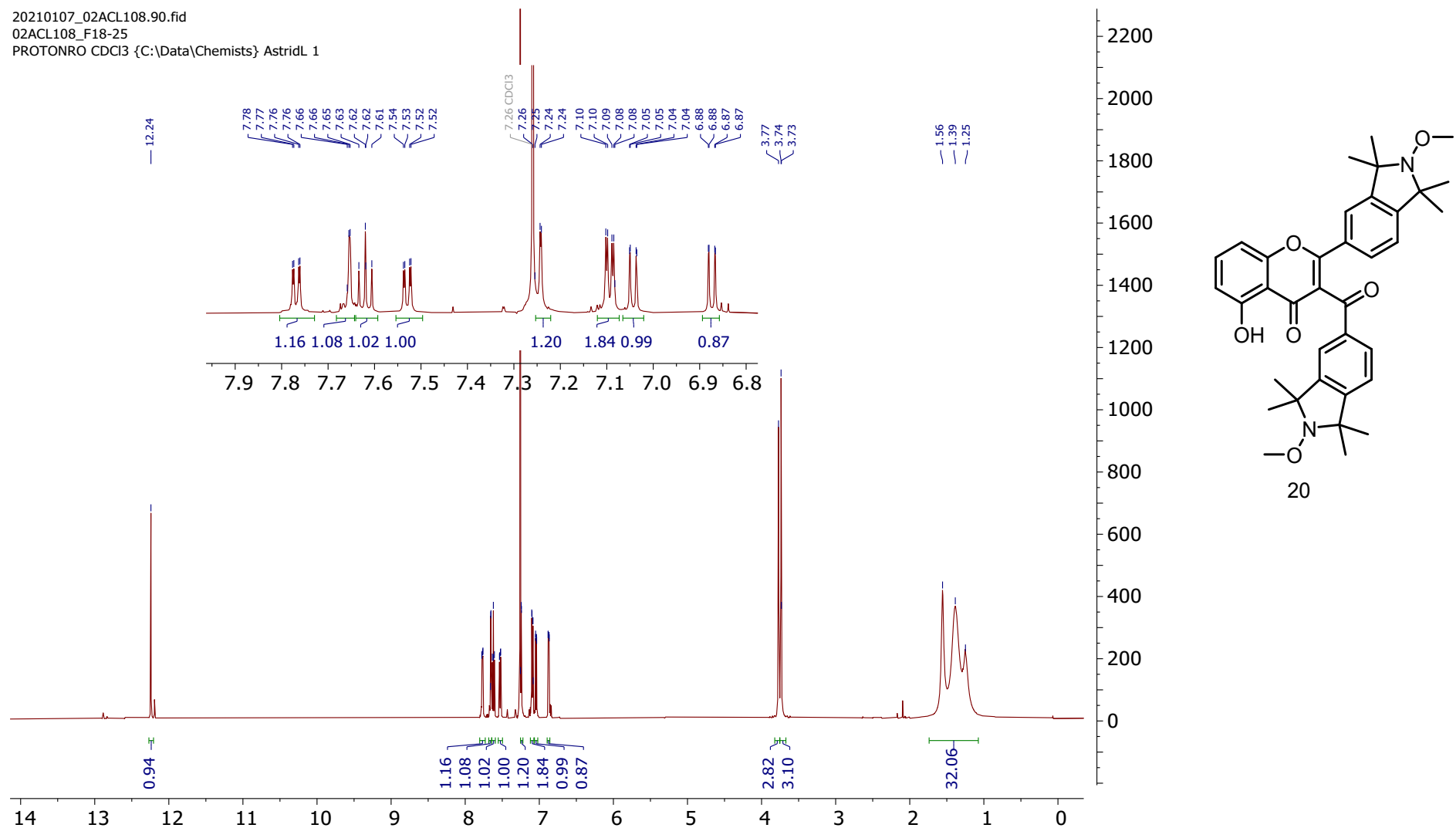


Figure S37: ¹H NMR spectra of **20** (CDCl₃, 600 MHz).

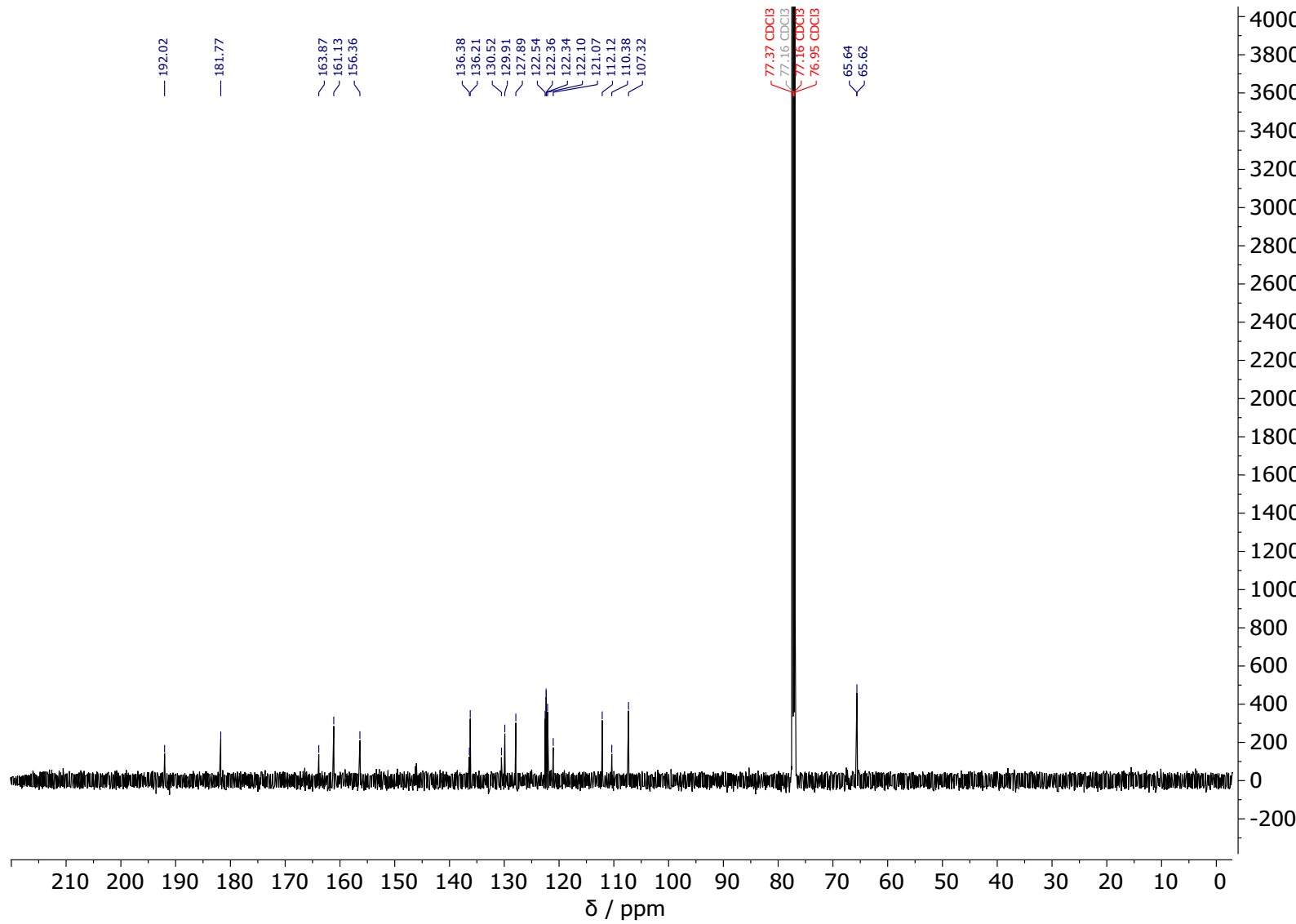


Figure S38: ^{13}C NMR spectrum of **20** (CDCl₃, 151 MHz).

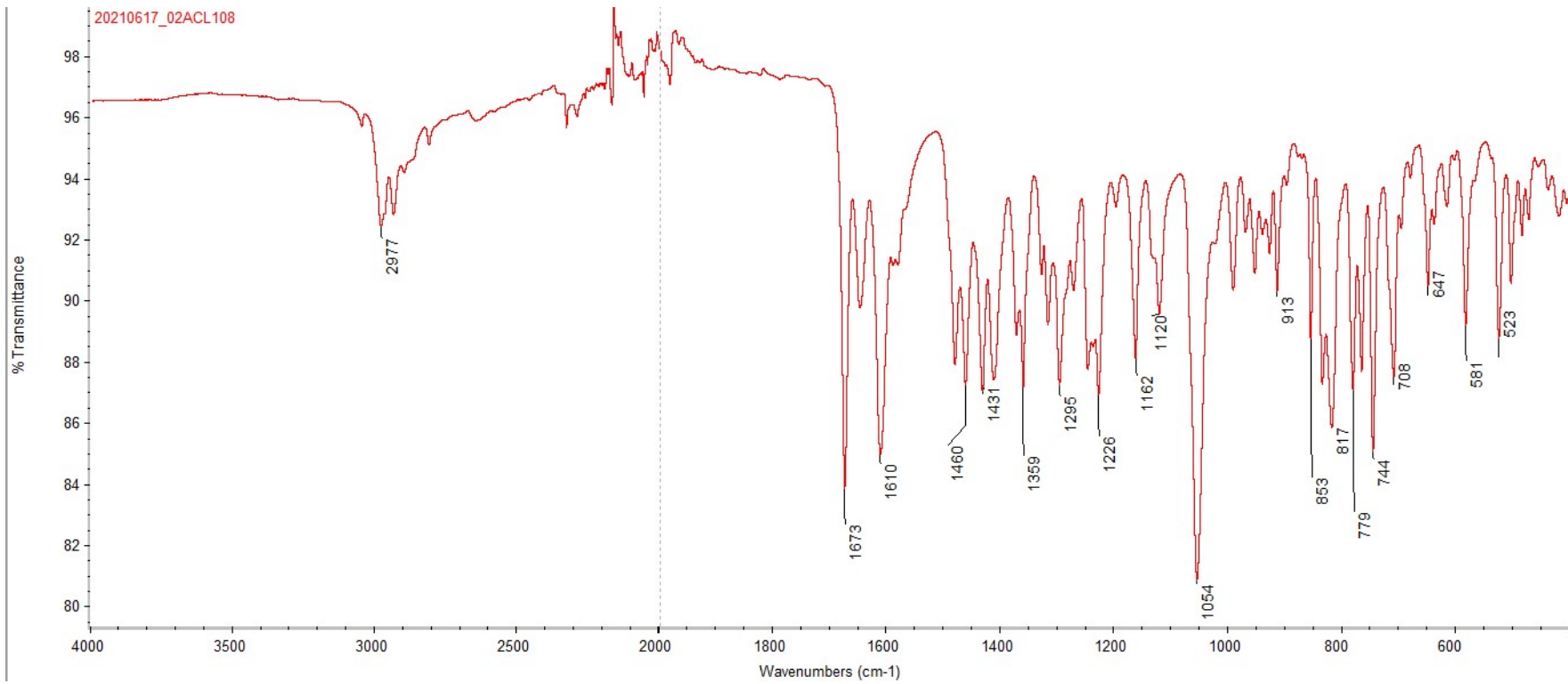


Figure S39: FT-IR spectrum of **20**

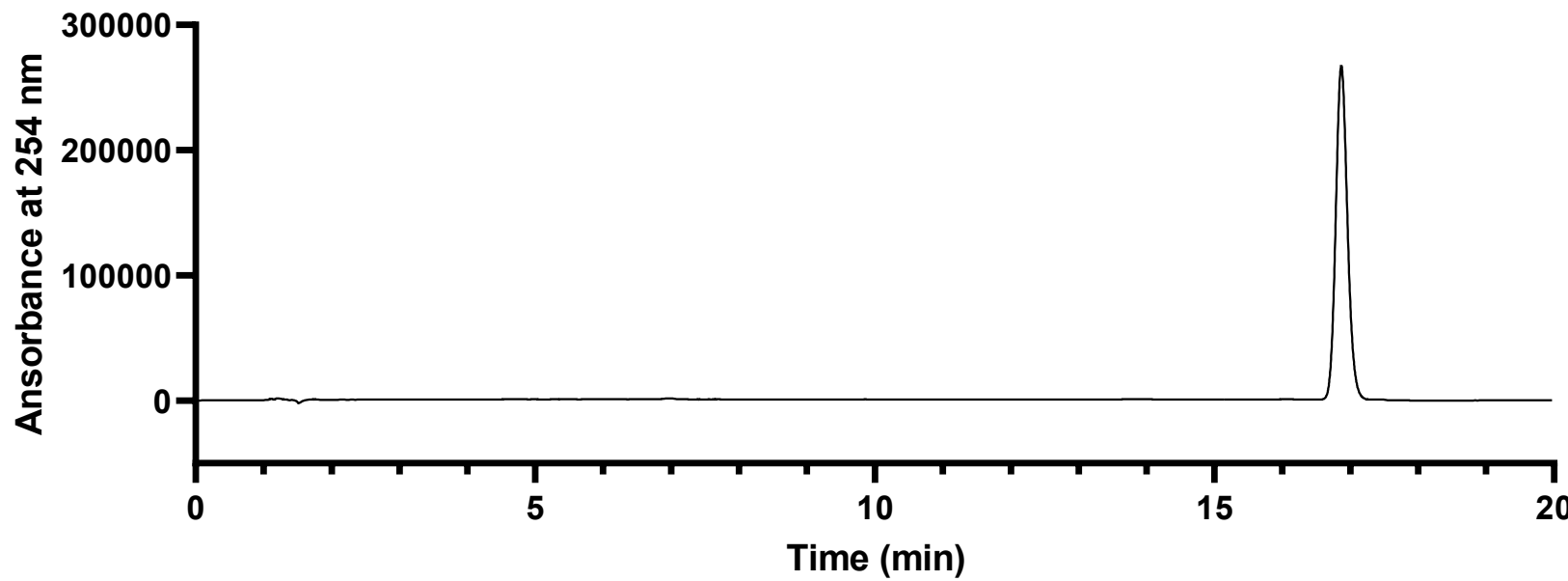


Figure S40: LC trace (254 nm detector wavelength) of **20**. The gradient was altered for this compound to ACN:H₂O (0.1% formic acid) 10:90 – 80:20.

5-Hydroxy-2-(1,1,3,3-tetramethylisoindolin-2-oxyl)-4H-chromen-4-one (7)

20210506_02ACL125.20.fid

02ACL125_F10-15

PROTONRO CDCl₃ {C:\Data\Chemists} AstridL 23

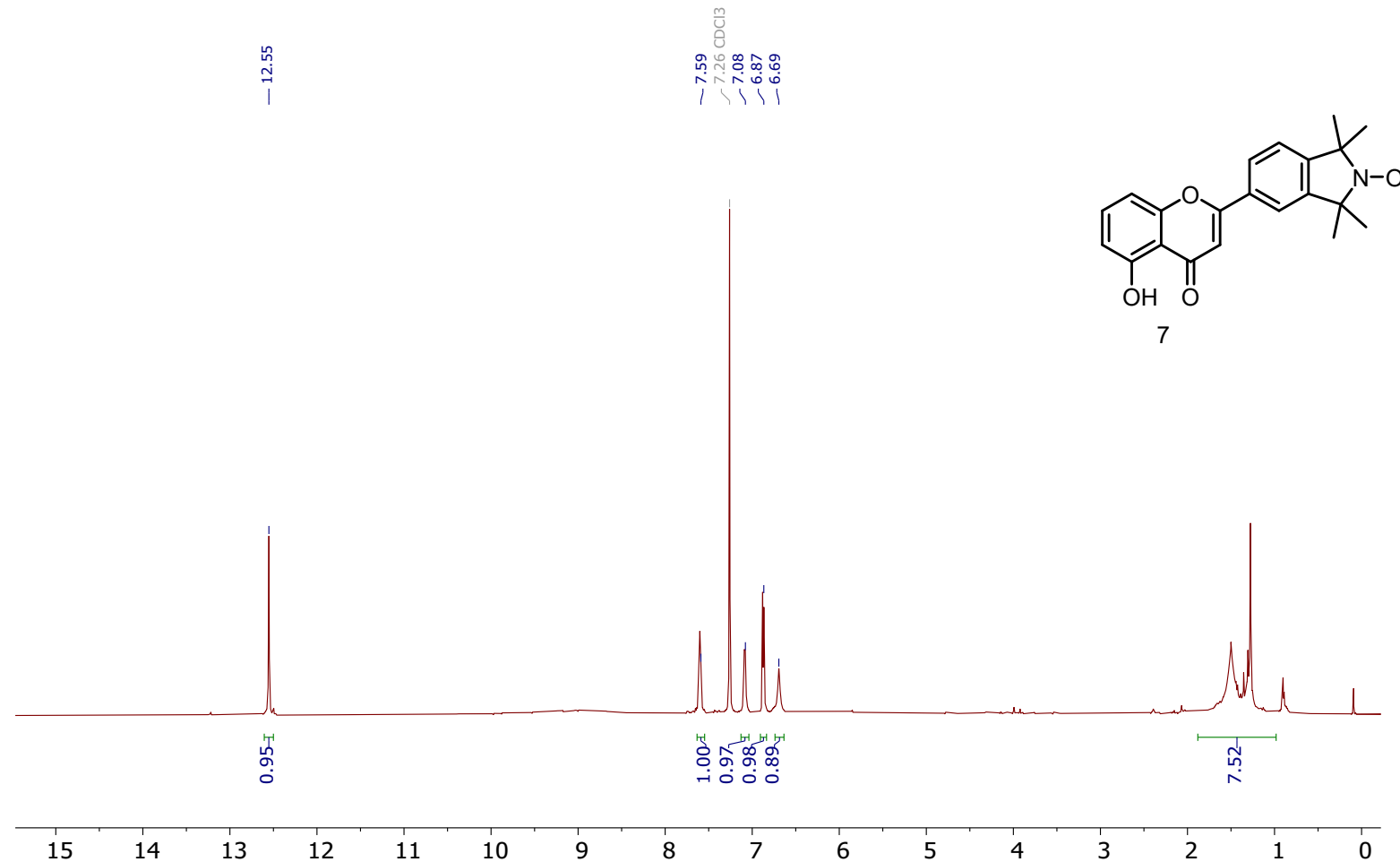


Figure S41: ¹H NMR spectra of **7** (CDCl₃, 600 MHz). Note: Nitroxide radicals often cause broad NMR signals, inaccurate integration, and missing integrals.

20210506_02ACL125.21.fid
02ACL125_F10-15
C13CPD CDCl₃ {C:\Data\Chemists} AstridL 23

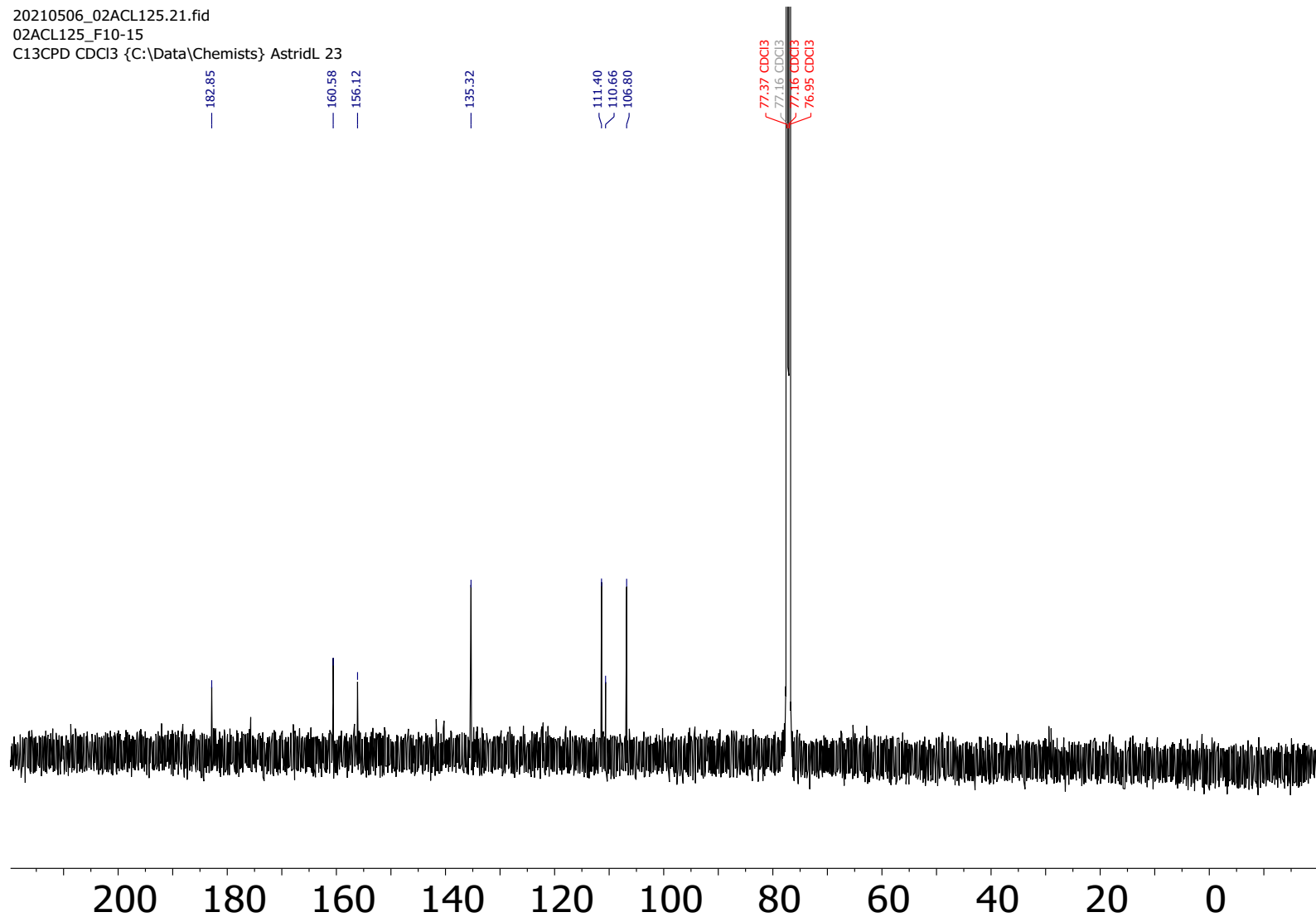


Figure S42: ¹³C NMR spectrum of **7** (CDCl₃, 151 MHz). Note: Nitroxide radicals often cause broad NMR signals, inaccurate integration, and missing integrals.

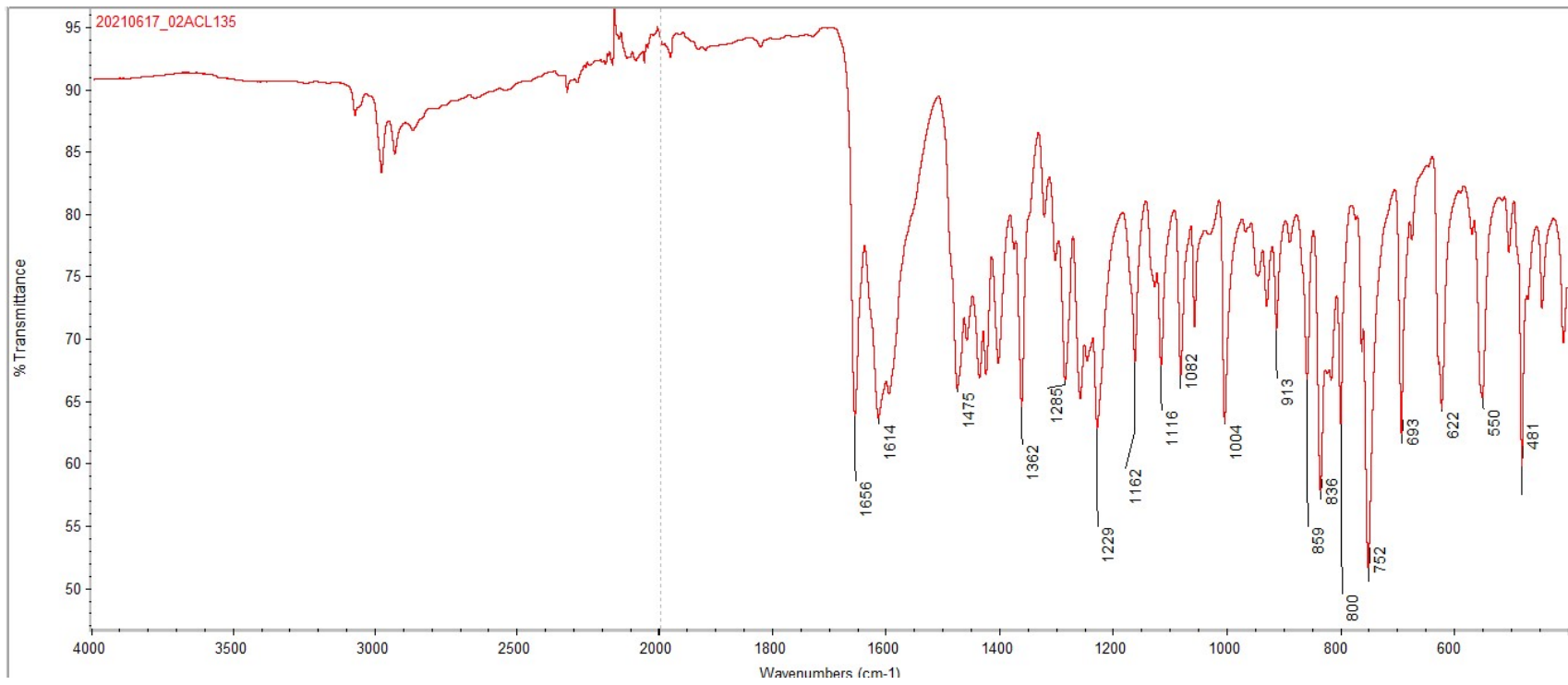


Figure S43: FT-IR spectrum of **7**

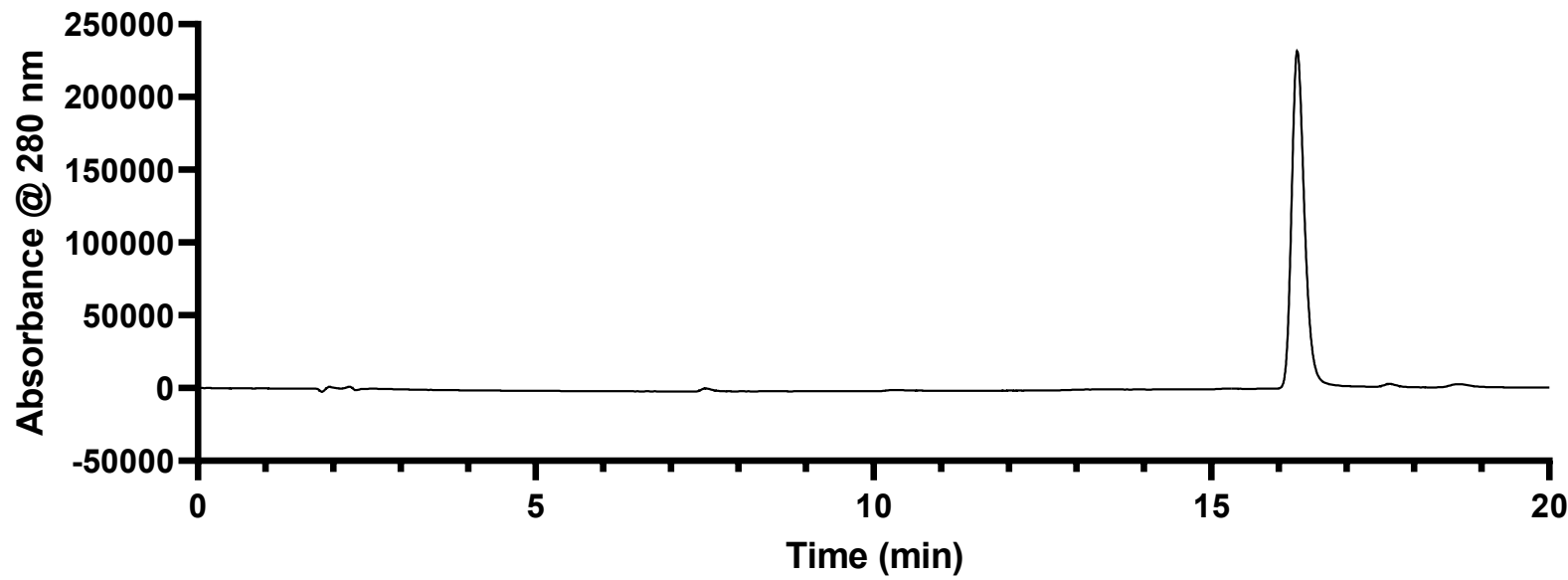


Figure S44: LC trace (280 nm detector wavelength) of **7**. The gradient was altered for this compound to ACN:H₂O (0.1% formic acid) 10:90 – 80:20.

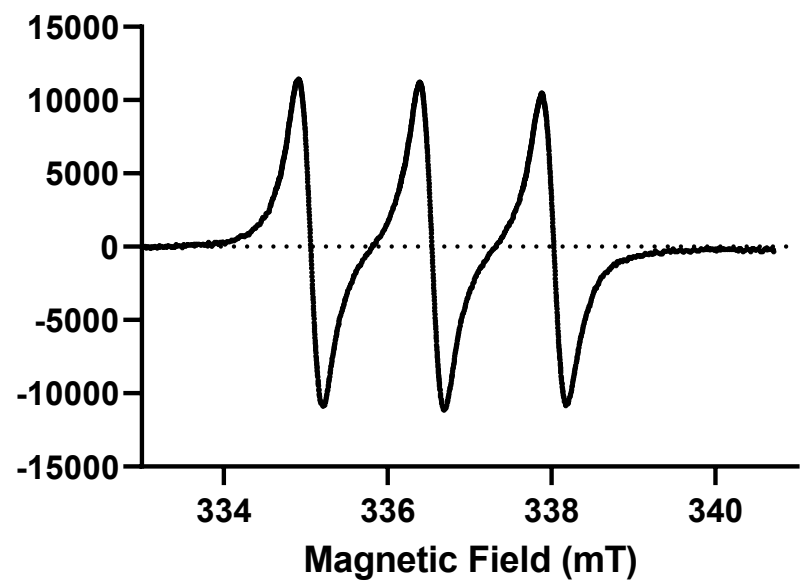


Figure S45: EPR spectrum of **7** in CDCl_3 ($a_N = 1.48 \text{ mT}$, $T = 298 \text{ K}$)

5-Hydroxy-2-(1,1,3,3-tetramethylisoindolin-2-oxyl)-3-(1,1,3,3-tetramethylisoindolin-2-oxyl-5-carbonyl)-4H-chromen-4-one (9)

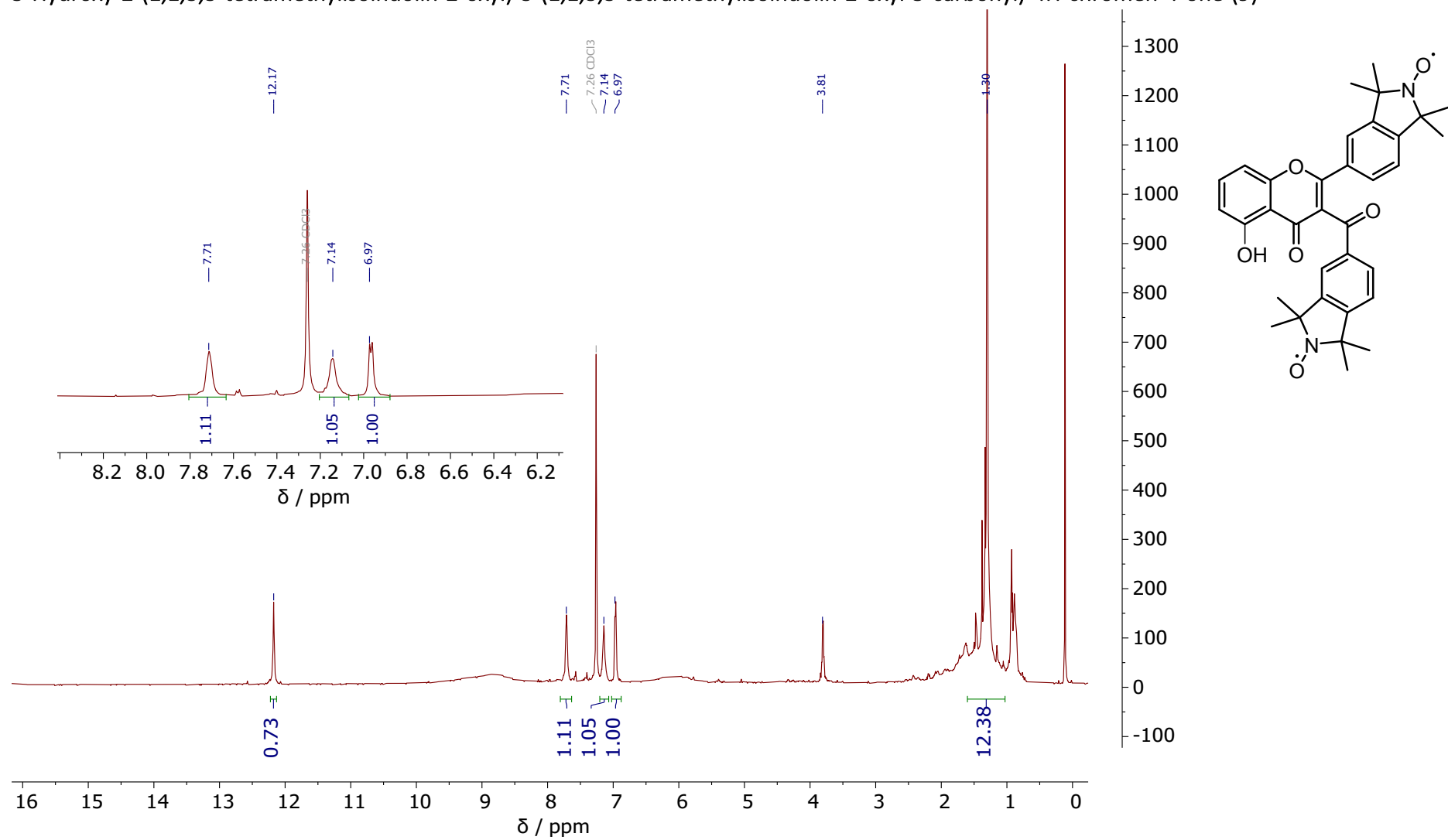


Figure S46: ^1H NMR spectrum of 9 (CDCl_3 , 600 MHz). Note: Nitroxide radicals often cause broad NMR signals, inaccurate integration, and missing integrals.

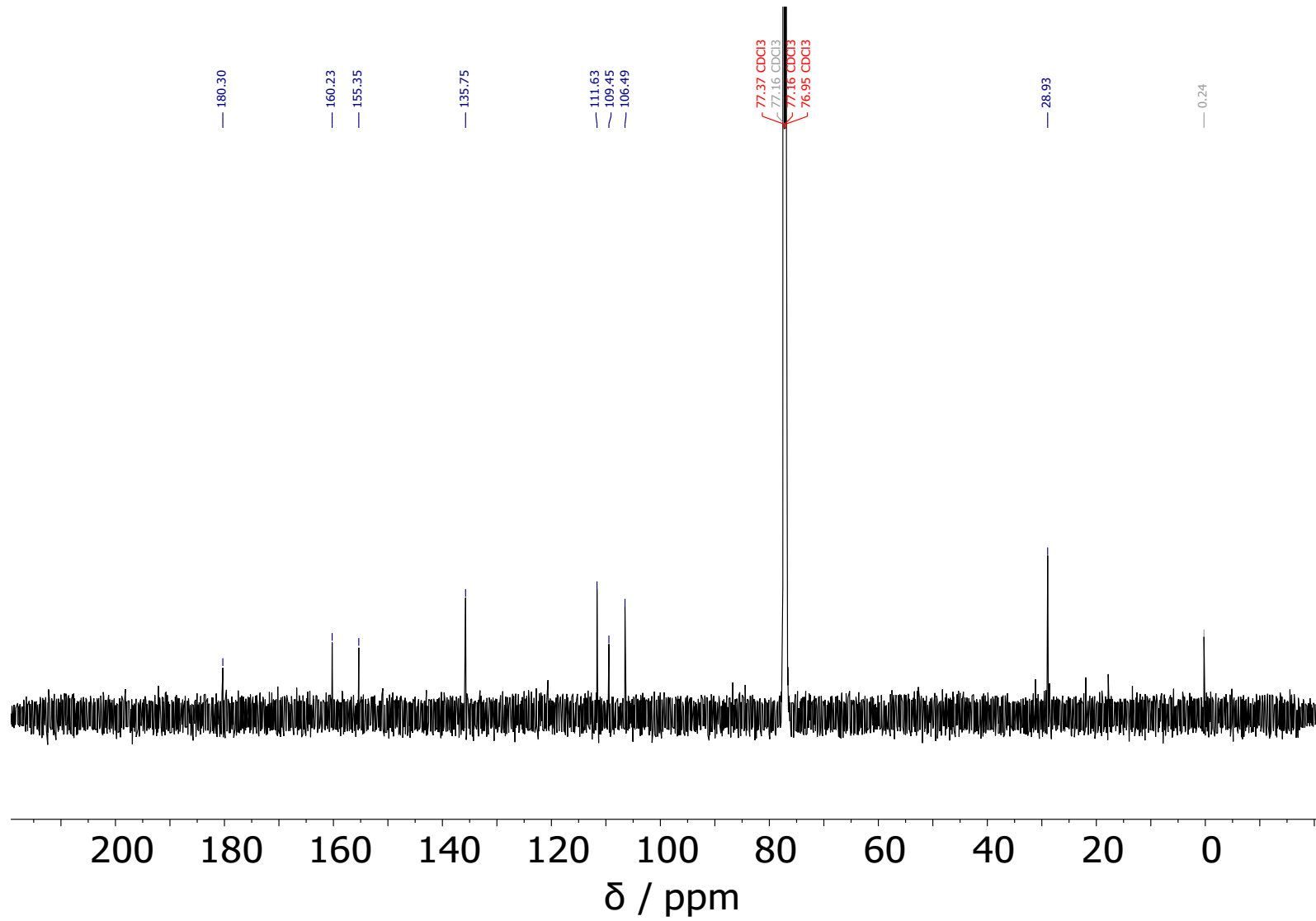


Figure S47: ^{13}C NMR spectrum of **9** (CDCl₃, 151 MHz). Note: Nitroxide radicals often cause broad NMR signals, inaccurate integration, and missing integrals.

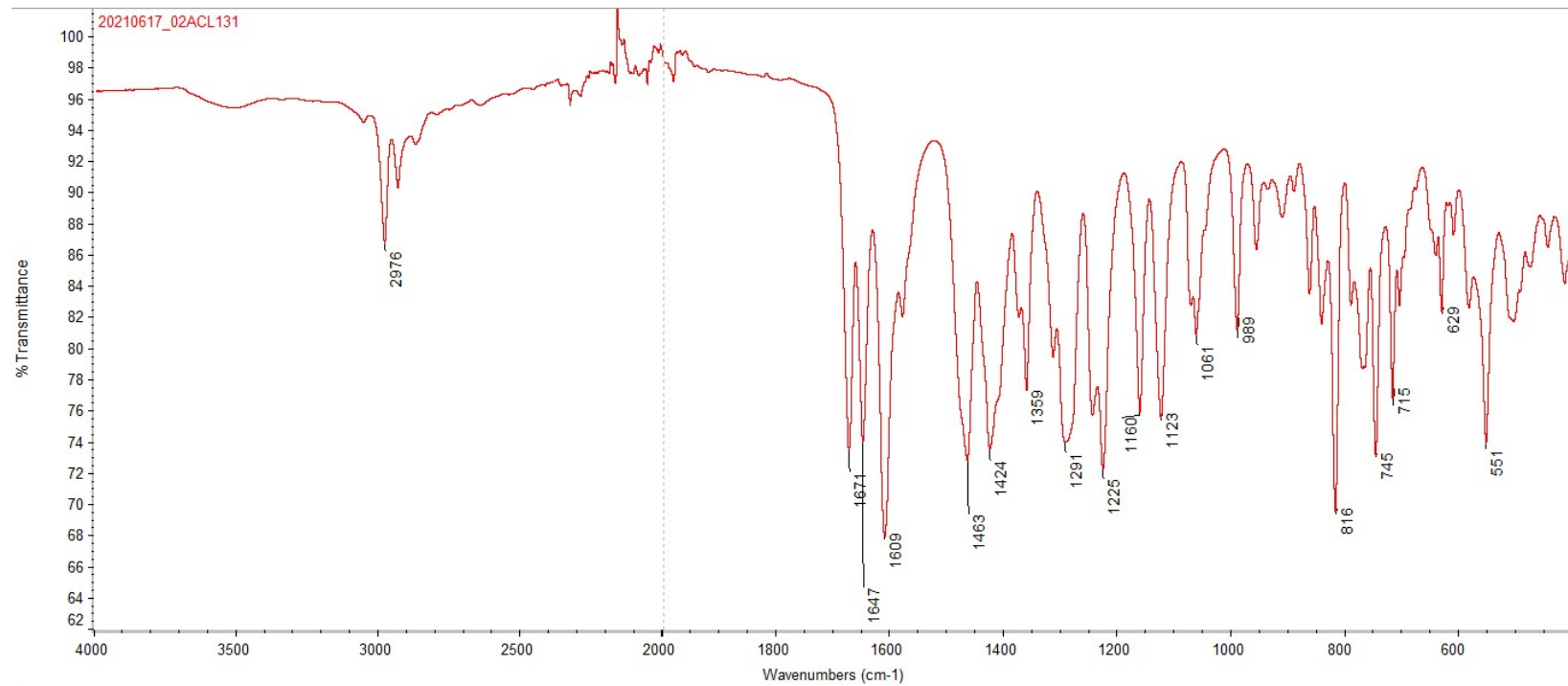


Figure S48: FT-IR spectrum of **9**

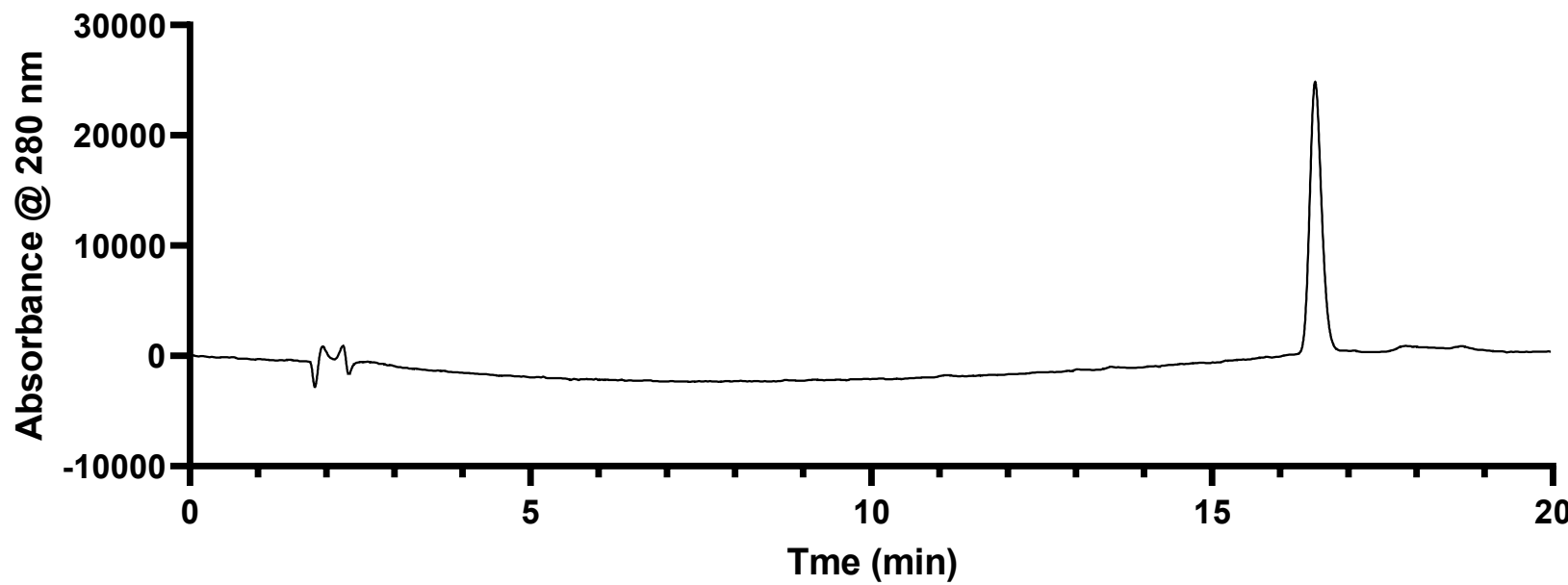


Figure S49: LC trace (280 nm detector wavelength) of **9**. The gradient was altered for this compound to ACN:H₂O (0.1% formic acid) 10:90 – 80:20.

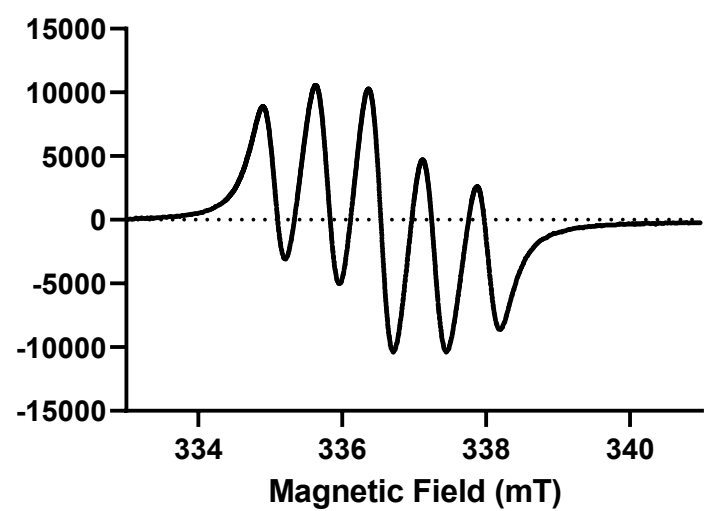


Figure S50: EPR spectrum of **9** in CDCl_3 ($a_N = 1.45 \text{ mT}$, $T = 298 \text{ K}$)

Single Crystal X-ray Diffraction Experimental

Single Crystal X-ray Diffraction (SCXRD) data were collected for **7**, **9** and **20** at the Australian Synchrotron MX2 beamline^[1] at 100(2) K using a wavelength of $\lambda = 0.7108 \text{ \AA}$. Synchrotron data acquisition was carried out using AS QEGUI^[2] and subsequent data indexation, reduction and integration was performed with XDS.^[3] Data for **18** were collected using a RigakuOD XtaLAB Synergy at 150(2) K with micro-focused MoK α radiation ($\lambda = 0.71073 \text{ \AA}$). Acquisition, indexation, reduction and integration for **18** were performed with the CrysAlis software package^[4] and a multi-scan absorption correction applied through the use of spherical harmonics, implemented in the SCALE 3 ABSPACK scaling algorithm. The structure was solved using SHELXT^[5] and subsequent modelling was carried out using SHELXL^[6] within the Olex2^[7] graphical user interface. Full occupancy non-hydrogen atoms were refined with anisotropic thermal displacement parameters, without applying rigid positional constraints. Disordered non-hydrogen atoms were modelled isotropically with occupancies refined through the use free variables. C–H hydrogen atoms were included in idealized positions and a riding model was used for their refinement. The positions of O–H hydrogen atoms were modelled using residual electron density present in the difference Fourier map along with a riding model. The O atom unique to the small component of oxidised product present in **20** (O4) was modelled anisotropically with an occupancy of 0.25 reflecting the residual electron density at this site. The CIF files have been deposited into the Cambridge Structural Database (reference numbers 2218184 - 2218187).

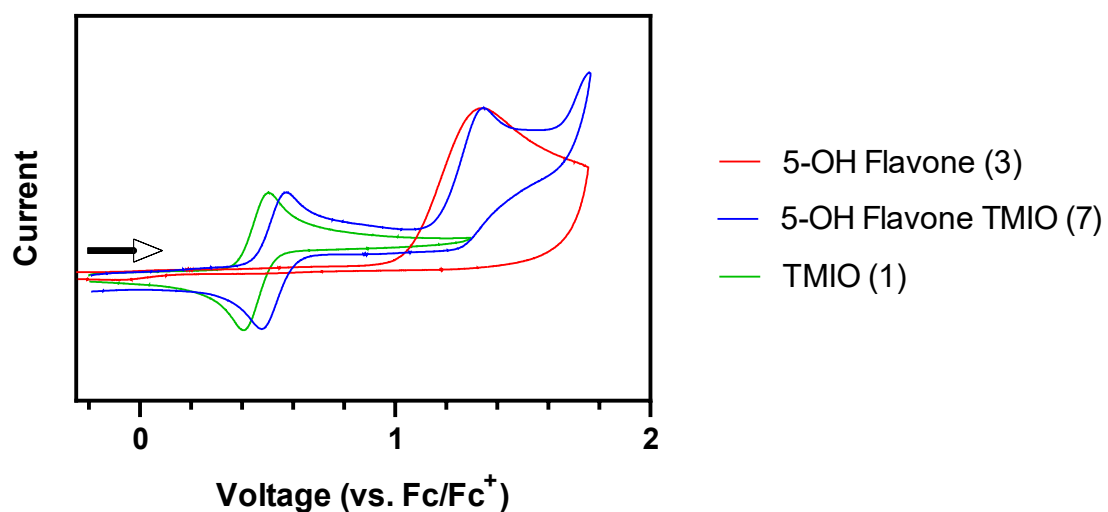
Table S1: Crystal and refinement data for **7**, **9**, **18** and **20**.

	7	9	18	20
Formula	C ₂₁ H ₂₀ NO ₄	C ₃₄ H ₃₄ N ₂ O ₆	C ₂₂ H ₂₃ NO ₄	(C ₃₆ H ₄₀ N ₂ O ₆) _{0.75} (C ₃₆ H ₃₉ N ₂ O ₇) _{0.25}
<i>M</i>	350.38	566.63	365.41	600.45
Crystal System	monoclinic	monoclinic	triclinic	Monoclinic
Space Group	P2 ₁ /c	P2 ₁	<i>P</i>	P2 ₁ /c
<i>a</i> / Å	6.8730(14)	8.6810(17)	5.8355(2)	10.664(2)
<i>b</i> / Å	20.799(4)	20.795(4)	11.8125(5)	34.087(7)
<i>c</i> / Å	12.761(3)	17.362(4)	14.5365(6)	8.8880(18)
α / °			110.197(4)	
β / °	104.29(3)	91.30(3)	96.116(3)	94.83(3)
γ / °			91.402(3)	
<i>V</i> / Å ³	1767.8(7)	3133.4(11)	933.04(7)	3219.4(11)
<i>D_c</i> / g cm ⁻³	1.316	1.201	1.301	1.239
<i>Z</i>	4	4	2	4
Size / mm	0.1 × 0.1 × 0.1	0.05 × 0.05 × 0.05	0.13 × 0.11 × 0.05	0.05 × 0.05 × 0.05
Colour	yellow	colourless	yellow	yellow
Crystal Habit	block	prism	block	prism
Temperature / K	100(2)	100(2)	150(2)	100(2)
λ / Å	0.7108	0.7108	0.71073	0.7108
μ / mm ⁻¹	0.091	0.083	0.089	0.085
<i>T</i> _{min,max}			0.66857, 1.00000	
2 <i>θ</i> _{max} / °	64.42	50.2	66.36	56.56
<i>hkl</i> range	-9 9, -29 29, -18 19	-10 10, -24 24, -20 20	-8 8, -17 17, -21 20	-14 14, -45 45, -11 11
<i>N</i>	31161	34216	21417	50607

$N_{\text{ind}} (R_{\text{merge}})$	5232(0.0312)	10534(0.0635)	5749(0.0489)	7954(0.0312)
$N_{\text{obs}} / (I > 2\sigma(I))$	4565	9046	4462	7441
N_{var}	240	768	250	418
$R1(F)^a, wR2(F2)^a$	0.0649, 0.2021	0.0801, 0.2280	0.0483, 0.1327	0.0623, 0.1762
GoF(all)	1.138	1.037	1.07	1.057
$\Delta\rho_{\text{min,max}} / \text{e}^{-\text{\AA}^{-3}}$	-0.260, 0.748	-0.468, 0.590	-0.259, 0.349	-0.801, 0.860
^a Reflections with [$I > 2\sigma(I)$] considered observed. $R1 = \sum F_o - F_c / \sum F_o $ for $F_o > 2\sigma(F_o)$ and $wR2_{(\text{all})} = \{\sum [w(F_o^2 - F_c^2)^2] / \sum [w(F_c^2)^2]\}^{1/2}$, where $w = 1/[\sigma^2(F_o^2) + (\mathbf{AP})^2 + \mathbf{BP}]$, $P = (F_o^2 + 2F_c^2)/3$.				

Cyclic voltammograms of 5-OH Flavone and 5-OH-3-Benzoyl flavone series

Cyclic Voltammogram of Flavone Series



Cyclic Voltammograms of 5-OH-Benzoyl Flavone Series

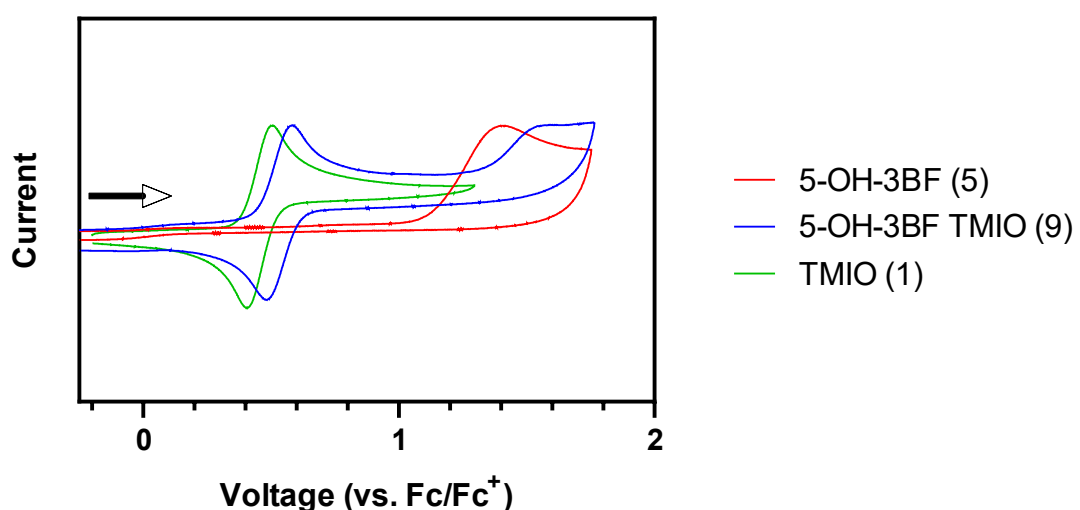
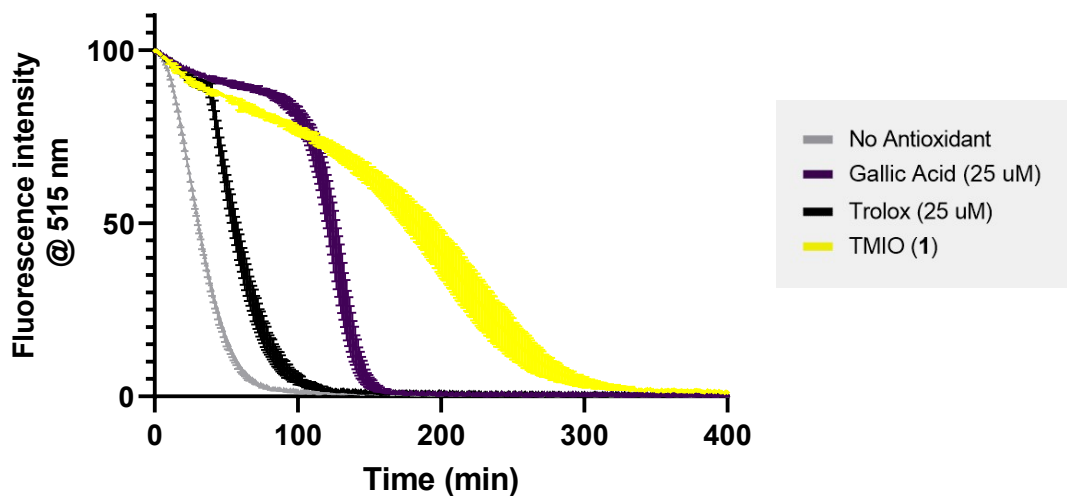


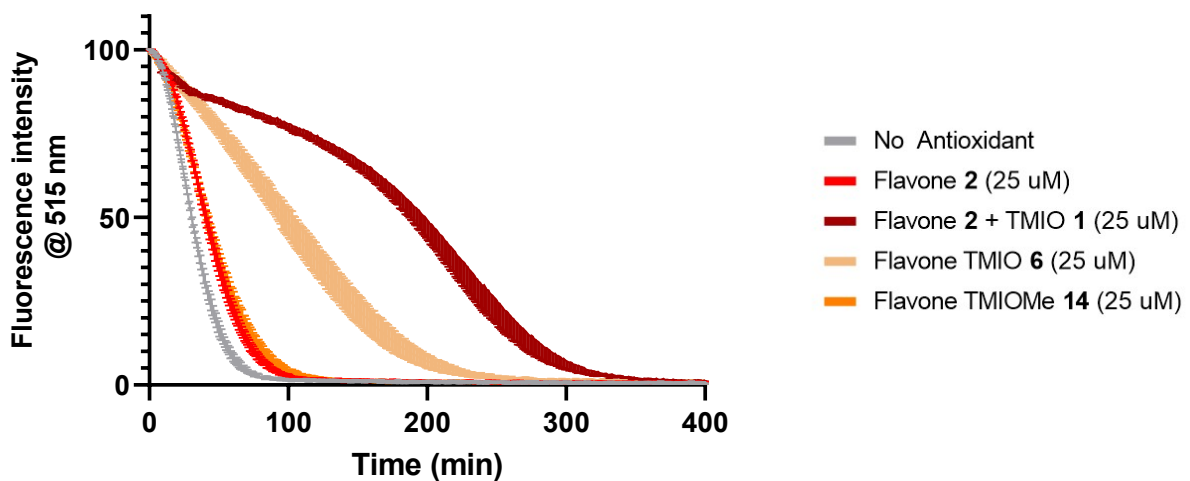
Figure S51: Cyclic Voltammograms of TMIO (1), hydroxylated flavones (3, 5) and hydroxylated flavone hybrids (7, 9) in ACN and Bu_4NPF_6 as supporting electrolyte. Voltammograms measured at a scan rate of 100 mV/s in the range of -0.5 – 2 V (vs. Ag/AgCl) and referenced to ferrocene/ferrocenium redox couple as internal standard. Current normalised between samples.

Oxygen Radical Antioxidant Capacity (ORAC) Data

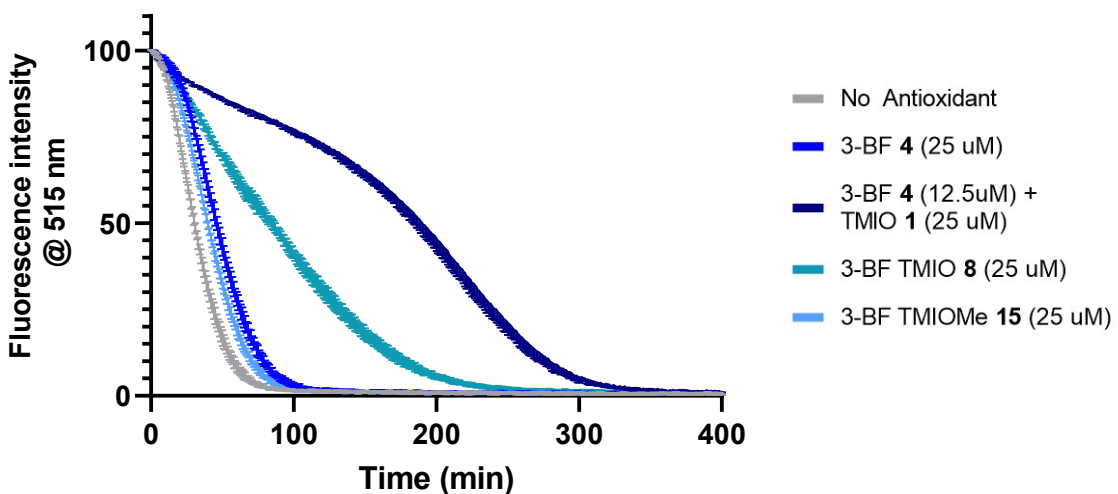
Positive Controls



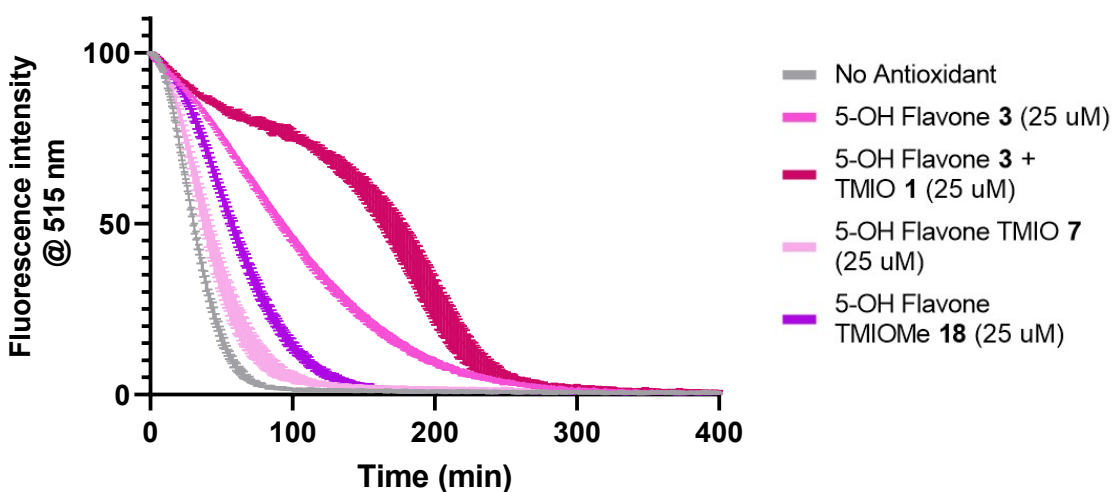
Flavone Series



3-Benzoyl Flavone Series



5-OH Flavone Series



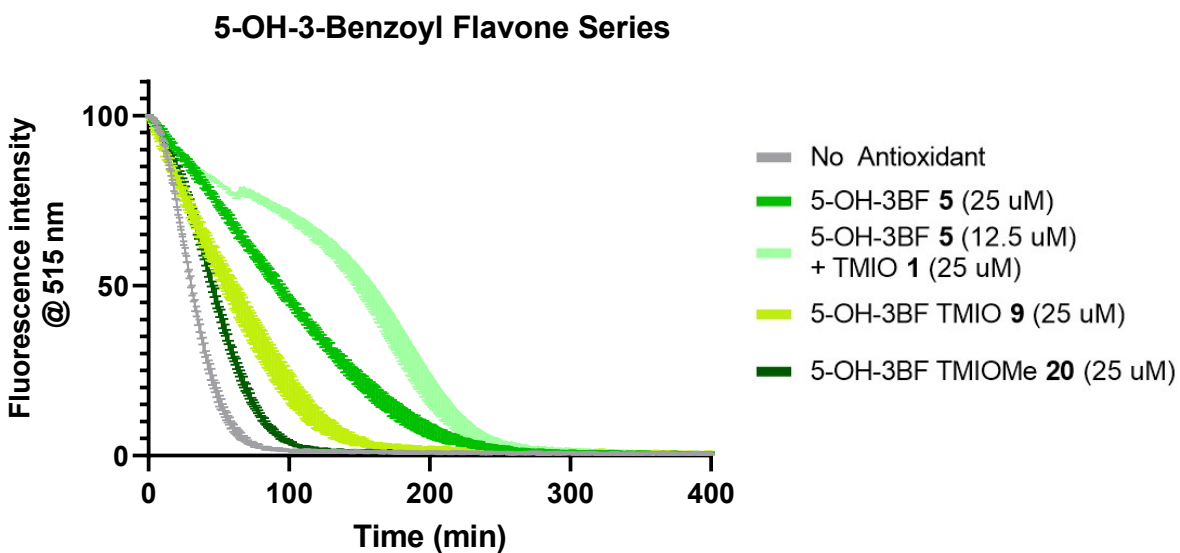


Figure S52: Fluorescence decay curves of samples in quadruplicate show as a fitted line including error bars of standard deviation at each time point. Samples include positive controls (Trolox, gallic acid and TMIO **1**), flavone series (**2**, **6**, **13** and **2+1**), 3-benzoyl flavone series (**4**, **8**, **15**, and **4+1**), 5-OH flavone series (**3**, **7**, **18**, and **3+1**) and 5-OH-3-benzoyl flavone series (**5**, **9**, **20** and **5+1**), compared to no antioxidant in the ORAC Assay.

Table S2: Area under the curve (AUC) and standard deviation (SD) of the quadruplicate fluorescence decay curve of each antioxidant sample in the ORAC assay. Net AUC = AUC_{Sample} - AUC_{no antioxidant}

Compound	AUC	SD	Net AUC	Net SD
No Antioxidant	3631	193	0	-
Trolox	6074	528	2443	562
Gallic Acid	11532	778	7901	802
TMIO (1)	17029	1022	13398	1040
Flavone (2)	4681	257	1050	321
Flavone TMIOMe (14)	4851	304	1220	390
Flavone (2) + TMIO (1)	18215	1161	14584	1177
Flavone TMIO (6)	10437	765	6806	790
3-BF (4)	5131	263	1500	326
3-BF TMIOMe (15)	4513	173	882	259
3-BF (4) + TMIO (1)	17658	613	14027	642
3-BF TMIO (9)	9434	312	5803	367
5-OH flavone (3)	10757	510	7126	545
5-OH Flavone TMIOMe (18)	6470	339	2839	326
5-OH Flavone (3) + TMIO (1)	15285	882	11654	642
5-OH Flavone TMIO (7)	4876	765	7126	611
5-OH BF (5)	10130	415	6499	458
5-OH BF TMIOMe (20)	5070	282	1439	342
5-OH BF (5) + TMIO (1)	14497	1366	10866	1380
5-OH BF TMIO (9)	6641	669	3010	696

ORAC assay followed by EPR and fluorescence spectroscopy

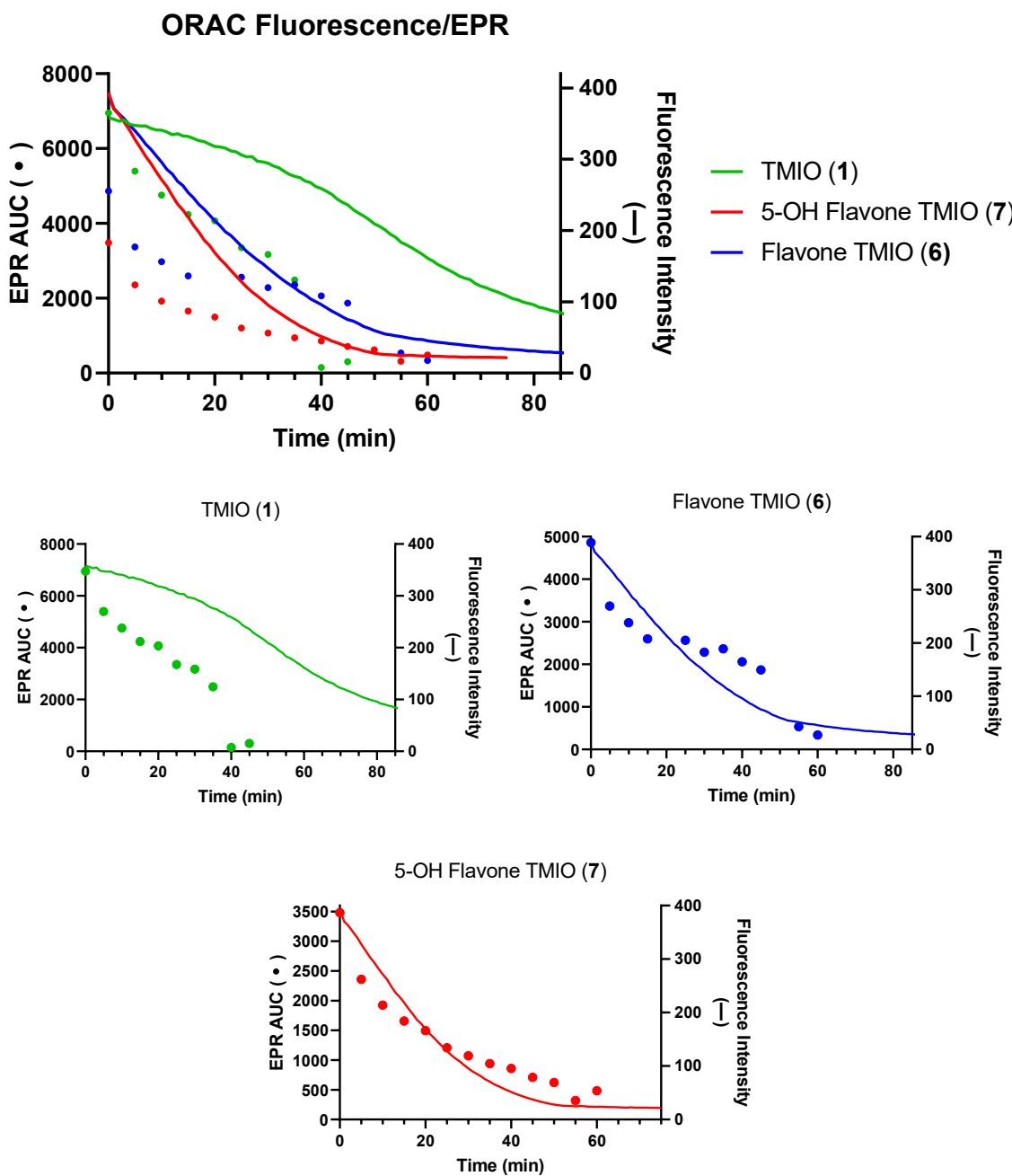


Figure S53: Scaled up ORAC assay measured by both fluorescence and EPR for 25 μM samples of TMIO (1), Flavone TMIO (6) and 5-OH Flavone TMIO (7). Double integral of the EPR spectra at 5-minute time points were taken and graphed on the left Y axis (dotted lined). Fluorescence intensity ($\lambda_{\text{ex}} = 485 \text{ nm}$, $\lambda_{\text{em}} = 515 \text{ nm}$) was measured every minute and graphed on the right Y axis (solid line).

EPR spectra of compounds (1, 6 and 7) in various solvents

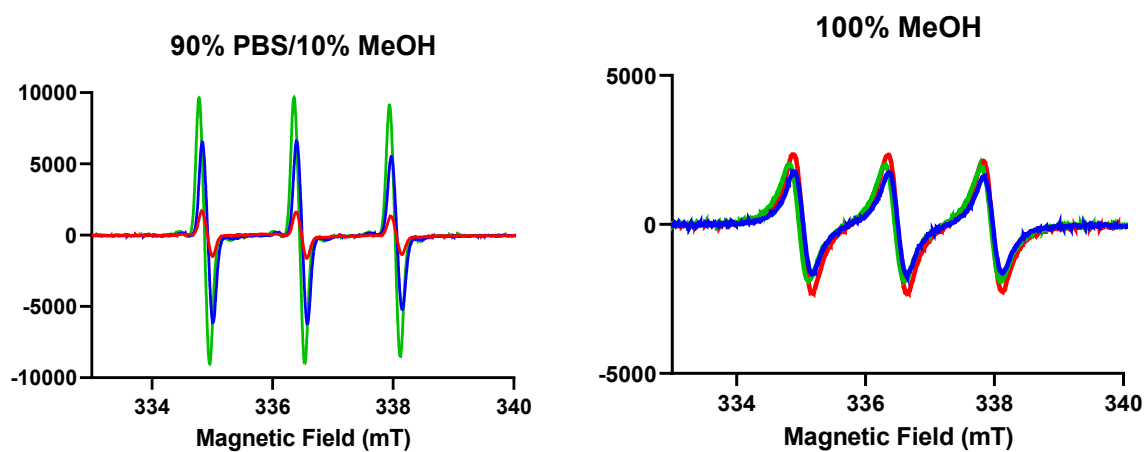


Figure S54: EPR spectra of TMIO **1** (green), Flavone – TMIO **6** (blue) and 5-OH Flavone TMIO **7** (red) (all 25 μ M) in various solvents ($T = 298$ K)

Table S3: Double integral of EPR spectra of TMIO **1**, Flavone – TMIO **6** and 5-OH Flavone TMIO **7** in various solvents (25 μ M)

Compound	90% PBS/10% MeOH	100% MeOH
TMIO (1)	7204	4007
Flavone-TMIO (6)	4951	3324
5-OH Flavone TMIO (7)	1443	4597

References

1. Aragao, D. et al. MX2: a high-flux undulator microfocus beamline serving both the chemical and macromolecular crystallography communities at the Australian Synchrotron. *J Synchrotron Radiat* **2018**, *25*, 885-891.
2. AS QEGui (<https://qtepics.github.io/>, 2019).
3. Kabsch, W. Automatic processing of rotation diffraction data from crystals of initially unknown symmetry and cell constants. *J. Appl. Cryst.* **1993**, *26*, 795-800.
4. *CrysAlisPro*; Agilent: Yarnton, Oxfordshire, England, **2014**.
5. Sheldrick, G. M. SHELXT – Integrated space-group crystal-structure determination. *Acta Crystallogr., Sect. A: Found. Adv.* **2015**, *71*, 3–8, DOI: 10.1107/S2053273314026370
6. Sheldrick, G. M. A short history of SHELX. *Acta Crystallogr., Sect. A: Found. Crystallogr.* **2008**, *64*, 112– 122, DOI: 10.1107/S0108767307043930
7. Dolomanov, O. V.; Bourhis, L. J.; Gildea, J. A.; Howard, J. A. K.; Puschmann, H. OLEX2: a complete structure solution, refinement and analysis program. *J. Appl. Crystallogr.* **2009**, *42*, 339– 341, DOI: 10.1107/S0021889808042726